Zootaxa 3760 (1): 001–038
www.mapress.com/zootaxa/

Article

ISSN 1175-5326 (print edition)
ZOOTAXA
ISSN 1175-5334 (online edition)

http://dx.doi.org/10.11646/zootaxa.3760.1.1
http://zoobank.org/urn:lsid:zoobank.org:pub:949EBA3E-5779-478C-9A6F-464E06908AAF

An integrative appraisal of the diversification in the Atlantic forest genus *Delomys* (Rodentia: Cricetidae: Sigmodontinae) with the description of a new species

PABLO RODRIGUES GONÇALVES[1,3] & JOÃO ALVES DE OLIVEIRA[2]

[1]*Núcleo em Ecologia e Desenvolvimento Socioambiental de Macaé (NUPEM), Universidade Federal do Rio de Janeiro, Macaé, RJ, Brazil 27971-550*
[2]*Departamento de Vertebrados, Museu Nacional, Universidade Federal do Rio de Janeiro, Rio de Janeiro, RJ, Brazil 20940-040*
[3]*Corresponding author. E-mail: prg@acd.ufrj.br*

Abstract

Recent taxonomic studies on Neotropical mammals have benefited from the use of genetic data to unravel and recognize species diversity in a number of genera, including the Atlantic forest endemic genus *Delomys*. However, the success of this approach depends on ability to link genetically identified lineages to species names based on voucher specimens that lack genetic data. Cytogenetic studies in the Atlantic forest endemic rodent genus *Delomys* have revealed two widespread karyotypes, 2n=72/FN=90 and 2n=82/FN=80, which have been respectively ascribed to *Delomys sublineatus* (Thomas, 1903) and *D. dorsalis* (Hensel, 1872). More recently, a third karyotype, 2n=82/FN=86, reported from specimens collected on two montaintops in southeastern Brazil, was interpreted as evidence for a third species, *D. collinus* Thomas, 1917. This nominal form had originally been described as a subspecies of *D. dorsalis* from Itatiaia, one of the mountain ranges where the third karyotype was later detected. The detection of two sympatric karyotypes at the type locality of *D. collinus* in the Itatiaia mountain range, Southeastern Brazil, prompted a reevaluation of the association of karyomorphs and species names. In this paper, we assessed the congruence of molecular (cytochrome *b*), cytogenetic and morphological characters, to diagnose the species in the genus, including data from recently collected series and type specimens. Our results indicate that the genetic and morphological patterns are largely congruent with the recognition of three species, each of which is karyotypically and morphologically diagnosable. Our morphological analyses of sympatric samples from Itatiaia refute the former association of the 2n=82/FN=86 karyotype with the holotype of *D. dorsalis collinus* (which is more similar to *D. dorsalis* with 2n=82/FN=80). Instead, we recognize and describe a new species for the 2n=82/FN=86 populations from the highest altitudinal zones of the Itatiaia and Caparaó mountains. The geographical variation in *D. dorsalis* is also explored and the status of *D. d. collinus* is discussed in the light of the molecular and morphological evidence. Finally, we discuss biogeographic hypotheses concerning the disjunct distributions of *D. dorsalis* and the new species.

Key words: Itatiaia, Caparaó, altitudinal gradient, speciation, geographic variation, karyotype

Introduction

The Neotropical subfamily Sigmodontinae is the most diverse clade of rodents of the family Cricetidae, comprising 83 genera and about 400 living species (Musser & Carleton 2005; Pine *et al.* 2012). Although sigmodontine rodents have been studied for more than two centuries, a substantial portion of their diversity has only recently been recognized. In the last twenty years (1992–2012) 74 new species have been named and described, corresponding to roughly 18% of the current species-level diversity of the group (Reeder *et al.* 2007; Paglia *et al.* 2012). A dozen genera and even a new tribe have also been erected to account for the phylogenetic diversity of the subfamily (Weksler *et al.* 2006; D'Elía *et al.* 2007; Percequillo *et al.* 2011; Pine *et al.* 2012). As those numbers suggest, the taxonomy of sigmodontine rodents has been a prolific and dynamic field, and the current rate of new species descriptions is comparable to those of the age of scientific discoveries in the 19th century, when a vast spectrum of the diversity of mammals still remained to be described. Renewed collecting efforts, larger scientific collections of poorly known taxa or from unexplored remote areas, and an increasing number of taxonomists have

Accepted by M. Weksler: 16 Dec. 2013; published: 30 Jan. 2014

contributed to the recent discovery of several new sigmodontines, but among the determinants of this wave of discoveries, is indeed the use of cytogenetic and molecular evidence to diagnose and delineate taxa (Costello *et al.* 2013). The accumulation of karyological and, especially, DNA sequence data for an increasing number of sigmodontines has allowed the direct study of genetic variation among populations and species at spatial and temporal scales that were intractable several decades ago.

Despite the obvious advantages of the application of genetic and molecular tools in mammalian taxonomy, this approach also depends on the unequivocal association of genetically defined clades or karyotypes with available scientific names. The use of genetic data is relatively recent, especially in Neotropical sigmodontine taxonomy, which has been traditionally based on voucher skins and/or skulls rarely associated with karyological or molecular information. Therefore, except when it is possible to obtain genetic material from type specimens, the association between molecular lineages or karyotypes and species names must rely on morphological criteria.

The rodent genus *Delomys*, one of 18 mammalian genera endemic to the Atlantic forests of southeastern Brazil state and northeastern Argentina, exemplifies an interesting case of taxonomic identification of genetic groups. In the latest taxonomic revision of the genus, Voss (1993) recognized two species, *Delomys sublineatus* (Thomas 1903) and *D. dorsalis* (Hensel 1872), each diagnosable by morphological characters and karyotypes, lumping three names as junior synonyms (*lechei*, *obscura* and *plebejus*) and provisionally recognizing *collinus* Thomas 1917 as a subspecies of *D. dorsalis*. Subsequent cytogenetic analyses of samples from the highest altitudinal zones of Caparaó and Itatiaia mountain ranges in the states of Minas Gerais and Rio de Janeiro revealed a new karyotype (Bonvicino & Geise 1995), suggesting the recognition of a third species in the genus. As the type specimen of *collinus* was collected in the Itatiaia mountain range, Bonvicino & Geise (1995) assigned this name to the new karyotype and elevated it to species status. Consequently, three species have been recognized in the recent literature (e.g. Musser & Carleton 2005): *D. dorsalis* with a diploid number (2n) of 82 chromosomes and fundamental number (FN) of 80, *D. collinus* with 2n=82 and FN=86; and *D. sublineatus* with 2n=72 and FN=90.

A complication in this taxonomic structure arose from the fact that the 2n=82/FN=80 and 2n=82/FN=86 karyotypes assigned with *D. dorsalis* and *D. collinus*, respectively, were later reported to occur in sympatry on Itatiaia (Geise *et al.* 2004). Given that no karyological data is available for the century-old type specimen of *D. collinus*, and that the karyotyped sympatric samples were not described morphologically or compared to the holotype, the association between karyotypes and species names remains to be established. Published evidence cannot refute the possibility that the 2n=82/FN=80 karyotype represents *collinus*, in which case *collinus* might be conspecific with *D. dorsalis* (as originally envisioned by Thomas 1917), leaving the 2n=82/FN=86 karyotype unnamed. Furthermore, the reported karyotypic differences, unaccompanied by complementary morphological and molecular evidence, are not compelling evidence of species distinction, inasmuch as similar variation has been documented within other sigmodontine species (e.g., Bonvicino *et al.* 2001). Therefore, an integrative analysis of genetic and morphological variation among the karyotypically distinct forms, including comparisons of voucher specimens with type material, is required to effectively test the hypothesis that *Delomys collinus* is a valid species from Southeastern Brazil.

In this paper we assess the number of species recognized in *Delomys* by evaluating the congruence among molecular, cytogenetic and morphological variation to diagnose the three species, including data from recently collected series and type specimens. By using this integrative framework, we provide evidence for the association of the type of *collinus* to samples with 2n=82/FN=80 rather than 2n=82/FN=86 karyotypes, based on a set of qualitative morphological characters. Given the taxonomic rearrangements proposed, a new species is described and the geographical variation and other taxonomically and biologically relevant information about this new species and *D. dorsalis* are summarized below. Finally, we discuss biogeographic hypotheses concerning the disjunct distributions of the new species and of *D. dorsalis*.

Material and methods

Analyzed specimens. We examined morphological characters in all voucher-specimens included in this study, totaling 520 specimens from 66 localities, which were assigned to 76 population samples (Figures 1 and 2, Appendix). Ten localities consisted of presumptive sympatric areas between either morphologically (*D. dorsalis* and *D. sublineatus*) or karyotypically (2n=82/FN=80 and 2n=82/FN=86) divergent forms. The specimens

examined consisted of skulls, postcranial skeletons, skins and fluid preserved material housed and catalogued at the following institutions: Natural History Museum, London, UK (BMNH); Field Museum of Natural History, Chicago, USA (FMNH); Museu de Biologia Mello Leitão, Santa Teresa, Brazil (MBML); Museu de História Natural Capão da Imbuia, Curitiba, Brazil (MHNCI); Museu Nacional, Rio de Janeiro, Brazil (MN); Museum of Vertebrate Zoology, University of California, Berkeley, USA (MVZ); Museu de Zoologia da Universidade de São Paulo, São Paulo, Brazil (MZUSP); Coleção de Mamíferos do Departamento de Zoologia, Universidade Federal de Minas Gerais, Belo Horizonte, Brazil (UFMG), and Museu de Zoologia João Moojen, Universidade Federal de Viçosa, Viçosa, Brazil (MZUFV). The series examined included the holotypes of *D. collinus* and *D. sublineatus*, and topotypes of *D. dorsalis* (from Taquara do Mundo Novo, Rio Grande do Sul state, Brazil) housed at the BMNH.

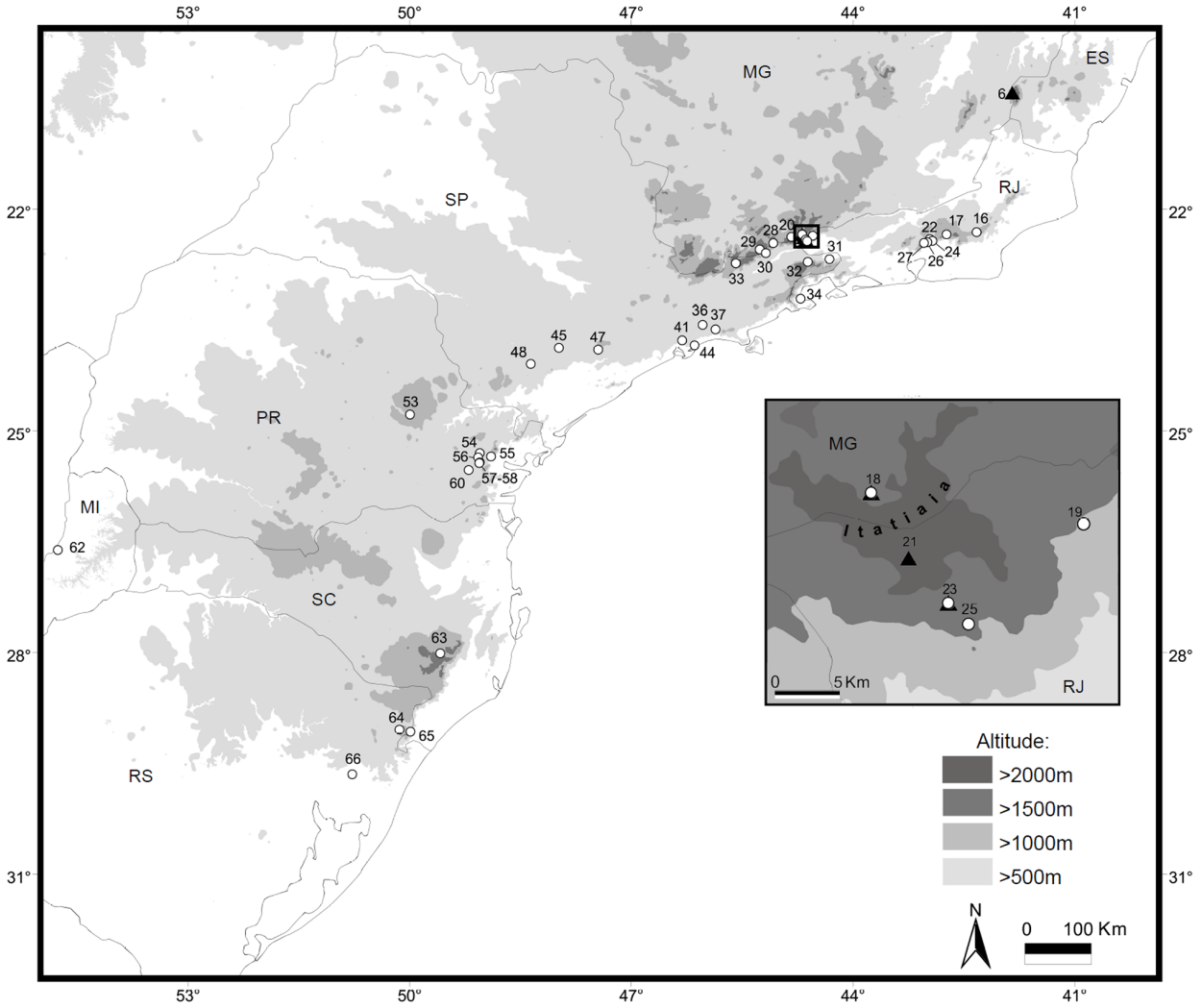

FIGURE 1. Collecting localities for specimens of *Delomys* **sp. nov.** (triangles) and *D. dorsalis* (circles) examined in this study. Localities from Mt. Itatiaia are highlighted in the inset. Acronyms refer to the Brazilian states of (ES) Espírito Santo, (MG) Minas Gerais, (RJ) Rio de Janeiro, (SP) São Paulo, (PR) Paraná, (SC) Santa Catarina and (RS) Rio Grande do Sul, and to the Argentinean province of Misiones (MI). All localities are listed in the Appendix.

Part of the recently collected samples were obtained by us in a series of expeditions throughout the Atlantic forests of southeastern and southern Brazil, mainly on montane areas with patches of humid montane forests and *campos de altitude* (Gonçalves *et al.* 2007). Taxonomically relevant material was obtained in two expeditions to different localities in the Itatiaia mountain range, within the limits of the Parque Nacional do Itatiaia, in Minas Gerais and Rio de Janeiro states. The first expedition was directed to the high-altitude locality known as "Campos do Itatiaia", a vast plateau at 2300–2500m altitude extensively covered by *campos de altitude*, and with narrow corridors of humid cloud forests along water courses. The second expedition focused on the eastward slope of the

Itatiaia mountain range, along the Maromba valley, at altitudes of 900 to 1400m, a region entirely covered by evergreen submontane and montane forests, where the type of *D. collinus* was supposedly obtained. Complementing our samples with voucher-specimens previously available in museums, we gathered a total of 46 specimens (25 of which were analyzed for *cytb* data) from four localities along the Itatiaia mountain range (localities 18, 21, 23 and 25 in Figure 1).

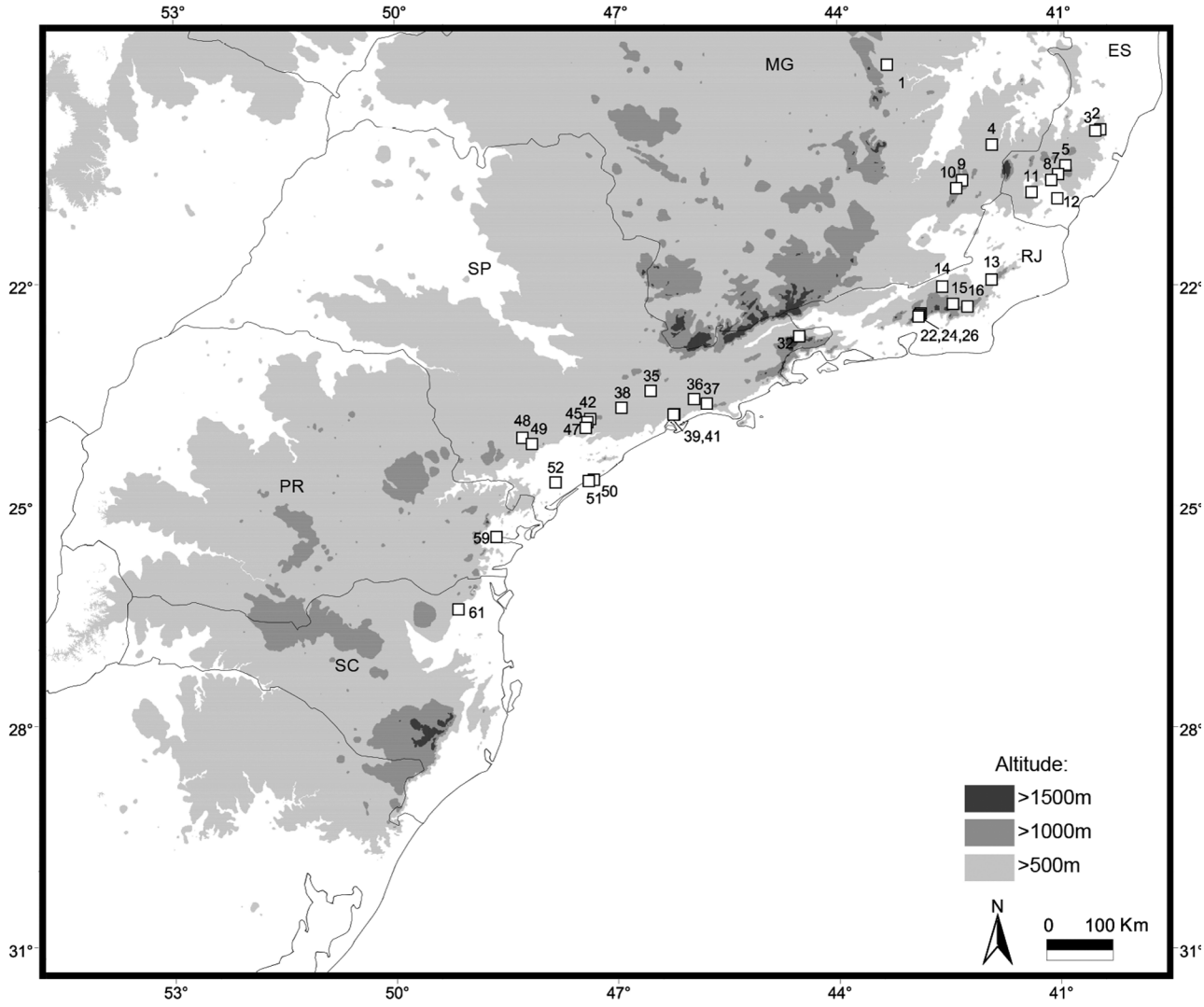

FIGURE 2. Collecting localities for specimens of *Delomys sublineatus* examined in this study. Acronyms refer to the Brazilian states of (ES) Espírito Santo, (MG) Minas Gerais, (RJ) Rio de Janeiro, (SP) São Paulo, (PR) Paraná, and (SC) Santa Catarina. All localities are listed in the Appendix.

Cytogenetic information. We compiled cytogenetic information for voucher-specimens not collected by us by reviewing the papers that explicitly associated those specimens with published karyotypes (Bonvicino & Geise 1995; Bonvicino *et al.* 1997; Geise *et al.* 2004) (Table 1). For some of these specimens, C. R. Bonvicino kindly allowed direct examination of cell suspensions and metaphase photographs to check diploid numbers and autosomal morphology of the specimens included in the analyses. The specimens collected by us were karyotyped following Ford & Hamerton (1956). We adopted the terminology of Levan *et al.* (1964) to identify chromosomal morphology. Fundamental number (FN) refers to the number of chromosomal arms of the autosomal complement.

Molecular data. We sequenced the mitochondrial cytochrome b gene (*cytb*) from 116 of the 520 specimens examined, representing 32 population samples from 28 localities covering the karyological diversity and most of the genus distribution (Table 1). Karyotypic information was directly available for 51 molecularly analyzed specimens (Appendix, Table A1).

TABLE 1. Samples of *Delomys* species genetically analyzed in this study. Sample sizes refer to number of specimens used in (*morph*) morphological and (*mtDNA*) molecular analyses. Other collecting localities are listed in Appendix and all samples are mapped on Fig. 1. Primary sources of karyotypes: 1– this study; 2– Bonvicino and Geise (1995); 3– Zanchin *et al.* (1992); 4– Geise *et al.* (2004); 5– Moreira *et al.* (2009).

Species	Locality	Alt. (m)	*morph*	*mtDNA*	Karyotype
Delomys sp. nov.	[6] Parque Nacional do Caparaó, Alto Caparaó, MG (Caparaó Mt.)	2500	13	8	2n=82; FN=86[1,2]
	[18] Brejo da Lapa, Itamonte, MG (Itatiaia Mt.)	1843	14	5	2n=82; FN=86[2,4]
	[21] Campos do Itatiaia (Abrigo Rebouças), Parque Nacional do Itatiaia, RJ (Itatiaia Mt.)	2450	3	2	2n=82; FN=86[1]
D. dorsalis	[17] Parque Estadual dos Três Picos, Salinas/Nova Friburgo, RJ	1600	7	7	2n=82; FN=80[1]
	[18] Brejo da Lapa, Itamonte, MG (Itatiaia Mt.)	1843	20	13	2n=82; FN=80[2,4]
	[19] Serrinha do Anambari, Itatiaia, RJ (Itatiaia Mt.)	850	1	1	–
	[25] Maromba, Itatiaia, RJ (Itatiaia Mt.)	1170	6	4	2n=82; FN=80[1]
	[26] Parque Nacional da Serra dos Órgãos (Paquequer), Teresópolis, RJ	1000	14	3	–
	[27] Parque Nacional da Serra dos Órgãos (Vale das Antas), Teresópolis, RJ	1950	11	3	–
	[28] Fazenda do Itaguaré, 10–16km SW Passa Quatro, MG	1500	5	2	–
	[29] Fazenda da Onça, 13km SW Delfim Moreira, MG	1850	2	2	–
	[31] Estação Ecológica do Bananal, Bananal, SP	800	2	2	–
	[32] Parque Nacional da Bocaina, São José do Barreiro, SP	1400	1	1	–
	[37] Estação Ecológica de Boracéia, Salesópolis, SP	850	54	6	2n=82; FN=80[3]
	[48] Parque Estadual Fazenda Intervales (Carmo base), Capão Bonito, SP	700	51	5	–
	[54] Parque Estadual Pico Paraná, Campina Grande do Sul, PR	1600	12	11	2n=82; FN=80[1]
	[57] Roça Nova, PR	950	17	5	–
	[58] Mananciais da Serra, Piraquara, PR	900	4	1	2n=82; FN=80[1]
	[63] Morro da Igreja, Urubici, SC	1700	2	2	2n=82; FN=80[1]
	[64] Parque Nacional Aparados da Serra, RS	1000	4	3	2n=82; FN=80[1]
	[65] Parque Nacional Serra Geral, Cambará do Sul, RS	1021	2	1	2n=82; FN=80[1]
D. sublineatus	[4] Mata do Sossego, Simonesia, MG	591	1	1	–
	[5] Sitio Pedreiras, Pedra Azul, Domingos Martins, ES	1000	1	1	–
	[9] Parque Estadual Serra do Brigadero (Fazenda Brigadeiro), MG	1200	3	2	2n=72; FN=90[5]
	[10] Parque Estadual Serra do Brigadeiro (Fazenda Neblina), MG	1300	10	5	2n=72; FN=90[5]
	[14] Sumidouro, RJ	1000	7	7	–
	[26] Parque Nacional da Serra dos Órgãos (base), Teresópolis, RJ	1200	3	1	–
	[32] Parque Nacional da Bocaina, São José do Barreiro, SP	1400	1	1	–
	[37] Estação Ecológica de Boracéia, Salesópolis, SP	935	7	4	2n=72; FN=90[5]
	[38] Caucaia do Alto (Reserva Morro Grande), SP	900	18	10	2n=72; FN=90[1]
	[49] Fazenda Sakamoto, Campinho, Capão Bonito, SP	932	2	2	–
	[52] Iguape, SP	3	3	2	–

Genomic DNA was isolated from ethanol-preserved liver tissue by the proteinase-K/phenol/clorophorm protocol (Sambrook *et al.* 1989) or the DNeasy DNA extraction kit following manufacturer instructions (QIAGEN Inc.). The quantity and quality of the total DNA was checked on 1% agarose gels.

The molecular phylogenetic data comprised either partial (801bp) or complete (1143bp) copies of the mitochondrial cytochrome *b* gene (*cytb*). The *cytb* gene copies were amplified in PCRs using the combinations of primers MVZ05 and MVZ16 (Smith & Patton 1993) for partial sequences and MVZ05 and CITBREV (Bonvicino *et al.* 2009) for complete sequences. Individual PCR reactions were prepared at final volumes of either 50µl or 25µl, containing final concentrations of 0.25µM of each primer, 7mM of $MgCl_2$, 10mM of dNTPs, 1x of PCR buffer, 250ng to 1µg of total DNA, and adding 0.2 to 0.4µl of Taq-Polimerase (QIAGEN or Taq-Platinum Invitrogen). The thermal protocol used for *cytb* PCRs consisted in 35 cycles with denaturation at 95°C for 1 min., annealing at 48°C for 1 min. and extension at 72°C for 1.5 min. The battery of cycles was preceded by prolonged denaturation at 95°C for 3 min. and succeeded by an additional extension at 72°C for 7 min. Negative controls were included in all reactions. The PCR products were checked in 1.5% agarose gels and purified for subsequent sequencing using the Qiaquick® PCR products purification kit (QIAGEN) or the GFX® PCR purification kit (GE Healthcare). Sequencing reactions included primers MVZ05, MEU1 (Bonvicino *et al.* 2009) and CITBREV, and were run in either MEGABACE 1000 or ABI 3730 automated sequencers (Applied Biosystems Inc.) or sent to the Macrogen International Sequencing platform (Macrogen Inc.). The sequence chromatograms were analyzed, edited and assembled using Chromas Pro 1.5 (Technelysium Inc.). In addition to the sequence data generated by us, we included *cytb* sequences of *Delomys dorsalis* and *D. sublineatus* kindly provided by J. L. Patton. All sequences were manually aligned and translated into aminoacids in MEGA 4.0 (Tamura *et al.* 2007) to check if the DNA sequences constituted orthologous open reading frames without unexpected stop codons. The sequences obtained and analyzed in this study were submitted to GenBank (Accession Numbers in the Appendix, Table A1).

Molecular evolutionary analyses. The *cytb* genealogies were estimated using maximum likelihood and Bayesian phylogenetic analyses implemented by softwares GARLI 2.0 (Zwickl 2006) and MrBayes 3.2 (Ronquist *et al.* 2012). Only unique haplotypes were submitted to phylogenetic analyses, avoiding an excess of zero length branches. Maximum likelihood analyses in GARLI 2.0 were run with 50 replicates of 100 random taxa addition sequences. We employed a General-Time-Reversible model with 6 substitution rates, unequal nucleotide frequencies, gamma distributed among-site substitution rate variation with four categories, and an estimated proportion of invariable sites (GTR+G+I), as selected using the Akaike information criterion in jModelTest 2.1.1 (Darriba *et al.* 2012). Node consistency was assessed through 1000 bootstrap iterations (Felsenstein 1985) with one search replicate per iteration, fixing the parameters of the GTR+I+G model to values previously estimated by the exhaustive search. In order to identify molecular synapomorphies of clades and/or species, joint reconstructions of ancestral nucleotide states were estimated using FastML (Ashkenazy *et al.* 2012) with the GTR model.

Bayesian phylogenetic analyses consisted in sampling the space of evolutionary trees and model parameters using a Monte Carlo Markov Chain (MCMC) procedure as implemented in MrBayes 3.2. The MCMC was run for 10 million generations in two independent runs with four parallel chains each, sampling topologies and model parameter values every 1000 generations, with swapping frequencies set to 1.0 and chain temperature to 0.2. The evolutionary model implemented in the Bayesian analyses was the same GTR+I+G used in likelihood analyses with parameter values set to be optimized during MCMC runs. The results were thoroughly checked for convergence examining the diagnostic parameters and checking for asymptotic behavior of the log-likelihood curves of the trees sampled throughout generations. The first 25% of the trees and parameters were discarded as "burn-in", and the remaining 75% of the trees were included in the sample used to estimate posterior probabilities of clades. All trees were rooted in the node uniting the neotomines *Neotoma* and *Scotinomys* to the sigmodontines *Sigmodon*, *Phyllotis* and *Delomys,* the last two genera always recovered as sister-groups in likelihood and Bayesian analyses. The selection of these genera as outgroups took into account the latest phylogenetic assessments of the Sigmodontinae based on combined nuclear and mitochondrial markers (Parada *et al.* 2013), which depict *Delomys* as sister to the tribe Phyllotini, and *Sigmodon* as the most basal genus in the Sigmodontinae tree.

Cytochrome *b* genetic distances have been useful as proximate descriptors of population and species level divergence in mammals (Baker & Bradley 2006). Therefore, pairwise genetic divergence between populations and species of *Delomys* were calculated using the uncorrected genetic *p*-distance in MEGA 4.0, expressed as percent sequence difference.

The levels of geographic structuring of genetic variation within species were examined qualitatively in

haplotype networks constructed by statistical parsimony using the software TCS 1.21 (Clement *et al.* 2000), and quantitatively by means of an analysis of molecular variance (AMOVA), using the software Arlequin 3.5 (Excoffier *et al.* 2005). In the AMOVA the total intraspecific pairwise variation between haplotypes was partitioned into three variance components and their respective Φ-statistics (analog to fixation indices or *F*-statistics): variance among geographic regions (Φ_{CT}), variance among populations within regions (Φ_{SC}) and variance within populations within regions (Φ_{ST}).

Morphological data and analyses. Morphological variation was assessed in quantitative and qualitative analyses of external, cranial and dental characters. In order to assess variation among individuals due to age, we classified specimens into four age categories defined by molar tooth wear (juvenile, subadult, adult and old-adult), and excluded the first two classes from morphological comparisons. Juvenile individuals exhibited third molars not fully erupted and with their occlusal surfaces not in the same plane as other molars. Subadults exhibited fully erupted third molars, but reduced wear in their occlusal surfaces and, consequently, a reduced area of exposed dentine. Adult individuals comprised the majority of specimens analyzed, being characterized by molars with marginal enamel folds, such as the mesoflexus/id and metaflexus/id, reduced to islands in first and second molars, leaving a well exposed area of dentine. Old specimens generally exhibited molars with enamel folds completely obliterated, flat cusps and occlusal surfaces that were completely flat due to advanced wear.

Our qualitative comparisons initially included examination of the set of external characters described by Voss (1993) to discriminate *D. dorsalis* and *D. sublineatus*, and then progressed to other external, cranial and dental traits that could be qualitatively described to account for the variation among species recognized by genetic evidence. The terminology used in the descriptions of integumental, cranial and dental characters follows Pardiñas (2008), Voss (1993), and Weksler (2006).

Our analyses of quantitative morphological variation among samples were based on a set of four external and 14 craniodental measurements registered in millimeters. The external measurements included head-and-body length (HBL), tail length (TL), ear length (EL) and hindfoot length (HFL), copied from the labels of voucher-specimens, except in the case of specimens collected by us, which were measured in the field prior to taxidermy as described by De Blase & Martin (1981). The following craniodental and mandibular measurements, described by Voss (1991) and Myers *et al.* (1990), were obtained with a digital caliper to the 0.01mm: condyloincisive length (CIL), greatest nasal length (NL), diastemal length (LD), length of the palatal bridge (LPB), antero-posterior length of the upper molar series measured at the crown (LM), greatest breath of M1 at the level of protocone-paracone (BM1), length of incisive foramen (LIF), breadth of rostrum at the level of the nasolacrimal capsules (BR), depth of rostrum at the level of the premaxillary-maxillary suture (DR), breadth of palatal bridge between the M1 protocones (BPB), breadth of the zygomatic plate at its mid-height (BZP), least interorbital breadth (LIB), braincase breadth (BB) measured just anterior to the squamosal-occipital suture and depth of braincase (DB) measured from the median base of the basisphenoid-basioccipital suture to the sagittal suture.

Multivariate patterns of craniometric variation among population samples were assessed by means of a Canonical Variate Analysis (Manly 1994), in order to depict the species and groups identified by genetic data in the multivariate craniometric space and to identify the most discriminant craniometric characters. We assessed confidence levels for classification of the individuals to their *a priori* identified groups on the basis of minimum Mahalanobis distances estimated in 1000 bootstrap resampling iterations. Only multivariate discrimination patterns with correct classification frequencies above 95% were considered statistically significant. We also inspected bivariate plots combining the most discriminant characters in order to validate the craniometric discontinuities among groups suggested by the Canonical Variate Analysis. All statistical computations for morphometric data were carried out in MatLab 4.2 (MathWorks, Inc.), using the function libraries developed by R. Strauss (1999).

Results

Molecular phylogenetics. Among the 116 specimens we sequenced, 87 unique haplotypes were recovered and submitted to phylogenetic analyses. The alignment of *Delomys* haplotypes with the outgroup sequences revealed a total of 468 variable sites, 231 of which are variable within the genus. The *cytb* genealogies recovered either by likelihood (best tree ln*L* = -6234.5797) or Bayesian analyses (sampled trees with mean ln*L* = -6367.3454) were highly congruent in depicting the genus *Delomys* as a monophyletic group containing three well-supported major clades (bootstrap support values > 75% and posterior probabilities > 90%) (Fig. 3). These three major clades are

coincident with the three karyotypes reported for species in the genus, two of them (2n=82/FN=80 and 2n=72/FN=90) more broadly distributed, and a third one (2n=82/FN=86) restricted to disjunct montane populations from the Itatiaia and Caparaó mountains (localities 6, 18 and 21). Therefore, the *cytb* molecular phylogeny is fully congruent with the karyological data in revealing three genetically exclusive species in the genus *Delomys*.

The karyotypes 2n=82/FN=80 and 2n=72/FN=90 were referred to *D. dorsalis* and *D. sublineatus*, respectively, by Zanchin *et al.* (1992). Since *Delomys sublineatus* and *D. dorsalis* are not sympatric at their respective type localities (localities 11 and 66, respectively), the karyotypes obtained from samples near these localities indeed corroborate the cytogenetic assignments previously made (Table 1). On the other hand, the nominal form *Delomys dorsalis collinus* Thomas, 1917 was referred by Bonvicino & Geise (1995) to specimens of the 2n=82/FN=86 clade, which are found in sympatry and even syntopy (locality 18, Fig. 1) with specimens of *D. dorsalis*. In the "Morphological Comparisons" section below we provide evidence to refute the assignment of *D. d. collinus* to specimens of the 2n=82/FN=86 clade, comparing these specimens to the holotype of *D. d. collinus* and genetically analyzed specimens of *D. dorsalis*. For now, we provisionally refer to the 2n=82/FN=86 clade as "*Delomys* **sp. nov.**" until its proper description in the "Species Accounts".

Molecular divergence among the three species is moderately high, ranging from 6.3% to 9.4% pairwise uncorrected genetic distance (Table 2). *Delomys dorsalis* and *Delomys* **sp. nov.** diverge by an average of 6.8% pairwise genetic distance, while *Delomys sublineatus* diverge from those two species by 8.6% and 8.3% average pairwise genetic distances, respectively. The maximum likelihood (ML) character reconstructions also reveal several apomorphic characters for *D. dorsalis* (at 24 sites), *Delomys* **sp. nov.** (at 28 sites) and *D. sublineatus* (at 37 sites), corroborating their recognition as well differentiated lineages.

TABLE 2. Percent pairwise genetic distance (*p*-distance) among species, among intraspecific lineages, and within species and intraspecific lineages (diagonal) in the genus *Delomys* based on cytochrome *b* gene sequences.

	Delomys **sp. nov.**	*D. dorsalis*			*D. sublineatus*
		Serra do Mar clade	Mantiqueira clade	Southern clade	
Delomys **sp. nov.**	0.33%				
D. dorsalis (Serra do Mar clade)	6.34%	0.64%			
D. dorsalis (Mantiqueira clade)	7.45%	4.80%	0.52%		
D. dorsalis (Southern clade)	6.75%	3.79%	3.72%	0.88%	
D. sublineatus	8.25%	7.72%	9.44%	8.61%	1.01%

The congruence between mitochondrial genealogies and karyotypes is further supported by the analyses of sympatric samples. Sympatric samples of *D. dorsalis* and *Delomys* **sp. nov.** at Brejo da Lapa (locality 18), in the Itatiaia mountain range, diverge by 6.6% sequence difference, while specimens in each species differ by only 0.3% sequence difference. Likewise, sympatric samples of *Delomys dorsalis* and *D. sublineatus* at Boraceia (locality 37) and Intervales (locality 48) also diverge by 7.7% to 8.4% genetic distance, while intraspecific divergence values at these localities range from 0.0% to 0.3%.

Despite the strong monophyletic status of these three species, their relationships are less clear. *Delomys* **sp. nov.** is recovered as a sister lineage to *D. dorsalis* in both Maximum Likelihood and Bayesian analyses, but without strong support (posterior probability = 0.69, bootstrap value < 50%). Likewise, the character optimization recovered only 10 synapomorphies uniting *Delomys* sp. nov and *D. dorsalis*.

Levels of intraspecific molecular variation differ substantially among the three species. Both in *Delomys* **sp. nov.** and in *D. sublineatus*, intraspecific divergence values are relatively low, with mean values not exceeding 1.1% of genetic distance. Some haplotypes of *D. sublineatus* are also shared among specimens from distant localities (haplotypes 66, 68 and 75, Fig. 3), contributing to a lack of reciprocal monophyly between geographic regions (Avise 2000), which suggests low levels of geographical subdivision. On the other hand, *Delomys dorsalis* exhibits high levels of intraspecific genetic divergence and a well-defined geographic structure, being subdivided into three geographic clades that are largely congruent with the distribution of three major mountain complexes in southeastern (Mantiqueira and Serra do Mar mountain ranges) and southern Brazil (Southern highlands) (Fig. 3). The Serra do Mar clade is constituted by samples in the coastal mountains of northeastern São Paulo and Rio de

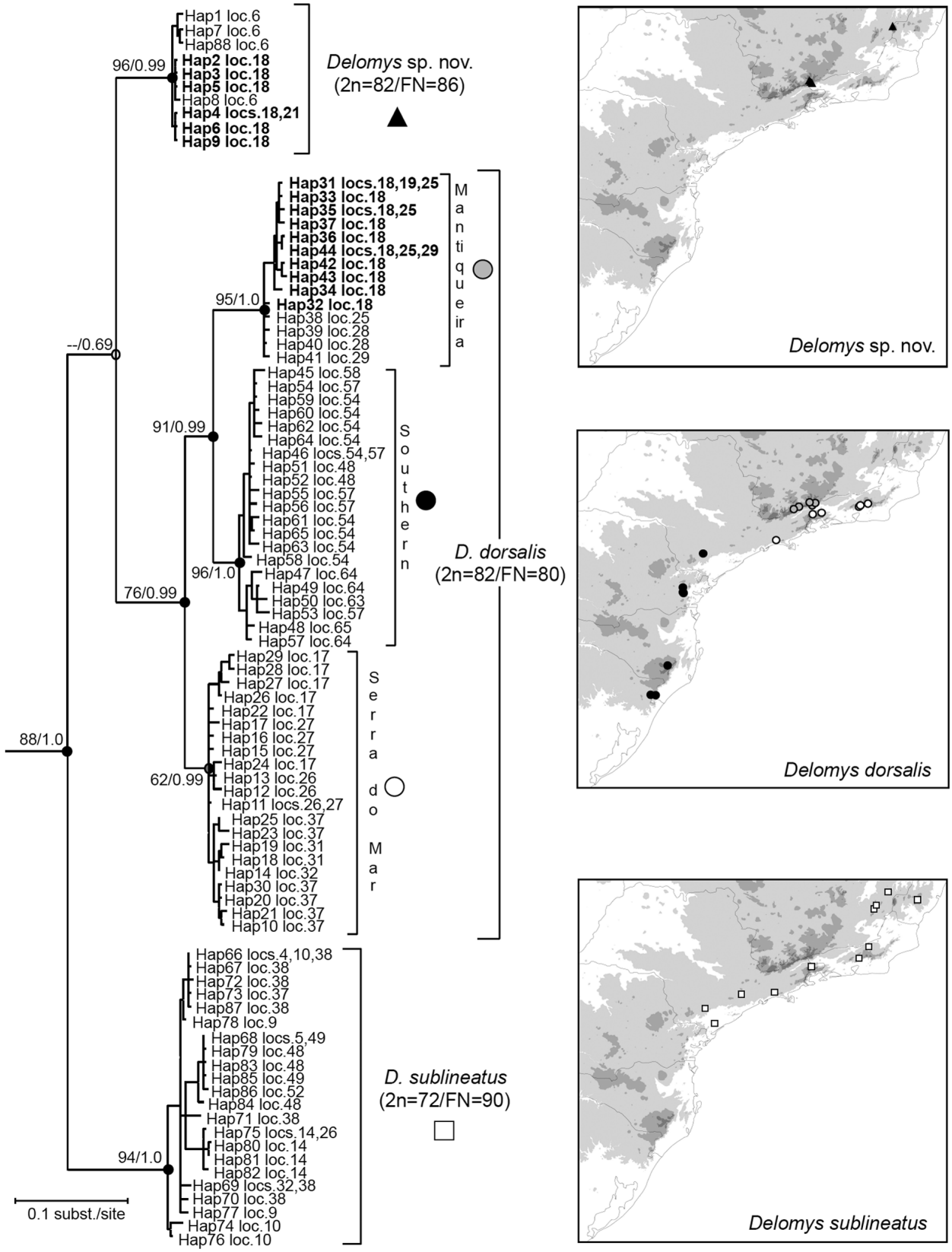

FIGURE 3. Phylogenetic relationships of cytochrome *b* haplotypes of species of *Delomys* with their respective karyotypes and geographic distributions of clades identified in the phylogeny. Haplotypes in bold occur sympatrically at the type locality of *D. d. collinus*. Numbers next to nodes refer to their bootstrap support values and posterior probabilities estimated in the maximum-likelihood and Bayesian phylogenetic analyses.

Janeiro states, while the Southern clade includes samples from the coastal mountains of southeastern São Paulo state and from along the Southern Highlands to the southernmost range of *D. dorsalis* in Rio Grande do Sul state. The Mantiqueira clade is restricted to the eastern range of Serra da Mantiqueira, which encompasses samples from the Itatiaia massif, and adjacent montane localities in São Paulo (Campos do Jordão, Piquete) and Minas Gerais (Delfim Moreira, Passa Quatro) states. The Mantiqueira and Southern clades of *D. dorsalis* are recovered as sister lineages, diverging from each other by 3.72% genetic distance and from the Serra do Mar clade by 3.79% to 4.8% genetic distance (Table 2). The mean divergence values within the three *D. dorsalis* clades are comparable to the intraspecific divergence levels found in *Delomys* **sp. nov.** and *D. sublineatus*, which range from 0.52% to 0.88% (Table 2).

Morphological comparisons: qualitative characters. Our qualitative morphological comparisons among *Delomys* **sp. nov.** and *D. dorsalis* are largely based on samples of genetically analyzed specimens from Itatiaia in order to recognize discrete character variation between these two species. This framework allowed us to test the allocation of the holotype of *D. dorsalis collinus* Thomas, 1917 (BMNH 14.2.23.12) to one of the two karyotypically divergent sympatric species based on morphological criteria. For these comparisons, we focused on distinctive characters that exhibited very limited geographic variation in *Delomys* **sp. nov.** and *D. dorsalis*, or were locally fixed in the Itatiaia populations of the two species. A summary of the distinctive characters among *Delomys* **sp. nov.**, *D. dorsalis* and *D. sublineatus* is provided in Table 3.

A first set of mandibular and cranial characters reveals unique and fixed conditions in *Delomys* **sp. nov.** that are useful to distinguish this species from *D. dorsalis*, *D. sublineatus* and the holotype of *D. d. collinus*. The mandibles of all specimens of *Delomys* **sp. nov.** exhibit a shallowly incised and broad sigmoid notch, and a reduced coronoid process, which connects to the condyloid process through a high bony ridge superior to the capsular process of the incisor alveolus (Fig. 4a). Conversely, the holotype of *D. d. collinus* and all adult specimens of the three clades of *D. dorsalis* display a much deeper and asymmetrically excavated sigmoid notch and a robust and well-pronounced coronoid process, which connects to the condyloid by a low bony ridge. *Delomys sublineatus* also exhibits a deep sigmoid notch, but considerably narrowed in relation to both *D. dorsalis* and *D. d. collinus* due to a more robust condyloid process. The angular process in *Delomys* **sp. nov.** is relatively reduced and does not project posteriorly beyond the limit of the condyloid process, while in *D. dorsalis* and *D. sublineatus* the angular process is more pronounced and projects beyond the limit of the condylar process. The angular processes of both mandibular rami of the *D. dorsalis collinus* holotype are broken, but the coronoid process and sigmoid notch conditions clearly suggest its higher similarity to *D. dorsalis* rather than to *Delomys* **sp. nov.** (Fig. 4a).

Variation in the sutures of the frontal with the squamosal and parietal in the supraorbital region also provides an important character for distinction of *Delomys* **sp. nov.** in relation to *D. dorsalis* and *D. d. collinus* (Fig. 4b). In all specimens of *Delomys* **sp. nov.** from Itatiaia and Caparaó, the frontoparietal and frontosquamosal sutures are continuous, as both the parietal and squamosal contact the frontal at the same level along the postorbital wall, leaving no area of dorsal contact between the frontal and squamosal (Fig. 4b). In the holotype of *D. d. collinus* and in all specimens of the three clades of *D. dorsalis* the frontosquamosal suture is anterior to the frontoparietal suture, forming an area of contact between the squamosal and the dorsal surface of the frontal. Some specimens of *D. sublineatus* display asymmetric conditions for this character, resembling the collinear condition of *D. altimontanus* in one side of the cranium but also displaying the typical condition of *D. dorsalis* on the other side. Nevertheless, most specimens of *D. sublineatus* display the same condition seen in *D. dorsalis* and *D. d. collinus* (Fig. 4b).

A second set of cranial characters displays some polymorphism in *D. dorsalis*, but exhibit rather fixed conditions in the Itatiaia populations of this species that are useful to distinguish it from sympatric *Delomys* **sp. nov.** The incisive foramina in *Delomys* **sp. nov.** from both Caparaó and Itatiaia mountain ranges have straight lateral outlines along their maxillary margins, being slightly curved only at their posterior limits (Fig. 5a). By contrast, the lateral outlines of the incisive foramina of *D. dorsalis*, *D. d. collinus* and *D. sublineatus* are more sharply curved along their maxillary margins, enclosing a more reduced area in the maxillary portion of the foramina (Fig. 5b–d). Polymorphism for this character could be found only in Southern populations of *D. dorsalis*, where some individuals exhibit conditions similar to those of *Delomys* **sp. nov.** The shape of the mesopterygoid fossa of the two populations of *Delomys* **sp. nov.** also differs from the widespread condition seen in the genus, being equally expanded at the level of the sphenopalatine vacuities and at its caudal portion along the pterygoid processes (Fig. 5a). In adult specimens of *Delomys dorsalis, D. d. collinus* and *D. sublineatus* with intact pterygoid processes the mesopterygoid fossa has its greater expansion at the level of sphenopalatine vacuities, but then conspicuously tapers caudally at the level of the pterygoid processes (Fig. 5b–d).

TABLE 3. Comparisons among *Delomys* sp. nov., the holotype of *D. dorsalis collinus*, *D. dorsalis* from Itatiaia and *D. sublineatus*. Fixed conditions exhibited by *Delomys* sp. nov. are italicized and unknown conditions are coded as "?".

Characters	***Delomys* sp. nov.**	***D. dorsalis collinus* (holotype)**	***D. dorsalis* (Itatiaia)**	***D. sublineatus***
1. Karyotype	*2n = 82; FN = 86*	?	2n = 82; FN = 80	2n = 72; FN = 90
2. Coronoid process in mandible	*Delicate*	Robust	Robust	Robust
3. Sigmoid notch in mandible	*Shallow, wide and symmetrically excavated*	Deep, wide and asymmetrically excavated	Deep, wide and asymmetrically excavated	Deep, narrow and asymmetrically excavated
4. Angular process in mandible	*Reduced and not projected beyond the posterior limit of condyloid process*	?	Pronounced and projected beyond the posterior limit of condyloid process	Pronounced and projected beyond the posterior limit of condyloid process
5. Frontoparietal and frontosquamosal sutures	*Collinear, without an area of dorsal contact between squamosal and frontal*	Discontinuous, with an area of dorsal contact between squamosal and frontal	Discontinuous, with an area of dorsal contact between squamosal and frontal	*Collinear* or discontinuous
6. Incisive foramina	*Straight lateral outlines along the maxillary portion*	Curved lateral outlines along the maxillary portion	Curved lateral outlines along the maxillary portion	Curved lateral outlines along the maxillary portion
7. Mesopterygoid fossa	*Equally expanded at its anterior and posterior portions*	Expanded only at its anterior portion	Expanded only at its anterior portion	Expanded only at its anterior portion
8. Nasal tube	*Well developed, projecting beyond the gnathic process*	*Well developed, projecting beyond gnathic process*	*Well developed, projecting beyond gnathic process*	Poorly developed, terminating at gnathic process
9. Body dorsal pelage texture and length	*Soft, dense and long*	*Soft, dense and long*	*Soft, dense and long*	Coarse and shorter
10. Mid-dorsal stripe	Ill-defined on most specimens (69%) and well-defined on few (31%)	Ill-defined	Well-defined on most specimens (74%) and ill-defined on few (26%)	Ill-defined on most specimens (64%) and well-defined on few (44%)

……continued on the next page

TABLE 3. (Continued).

Characters	*Delomys* sp. nov.	*D. dorsalis collinus* (holotype)	*D. dorsalis* (Itatiaia)	*D. sublineatus*
11. Lateral line of bright yellow hairs	*Absent*	*Absent*	*Absent*	Present
12. Hindfeet dorsal pelage	*Buffy or soiled, covered by dark-based hairs*	*Buffy or soiled, covered by dark-based hairs*	*Buffy or soiled, covered by dark-based hairs*	Whitish, covered by entirely white hairs
13. Mammae number and formula	*6 (0/2/2/2)*	*6 (0/2/2/2)**	*6 (0/2/2/2)*	8 (2/2/2/2)
14. Tail color pattern	*Strongly bicolor with pale venter throughout the proximal two-thirds of tail*	Weakly bicolor, with pale venter restricted to the proximal third of tail	Weakly bicolor, with pale venter restricted to the proximal third of tail	*Strongly bicolor, with paler venter throughout the proximal two-thirds of tail*
15. Upper M1	*Very asymmetrical anterolingual and anterolabial conules*	Less asymmetrical anterolingual and anterolabial conules	Less asymmetrical anterolingual and anterolabial conules	Less asymmetrical anterolingual and anterolabial conules
16. Lower m1	*Deeper protoflexid and diagonally oriented protolophid*	?	Shallow protoflexid and transversally oriented protolophid	Shallow protoflexid and transversally oriented protolophid

* - Female BMNH14.2.23.

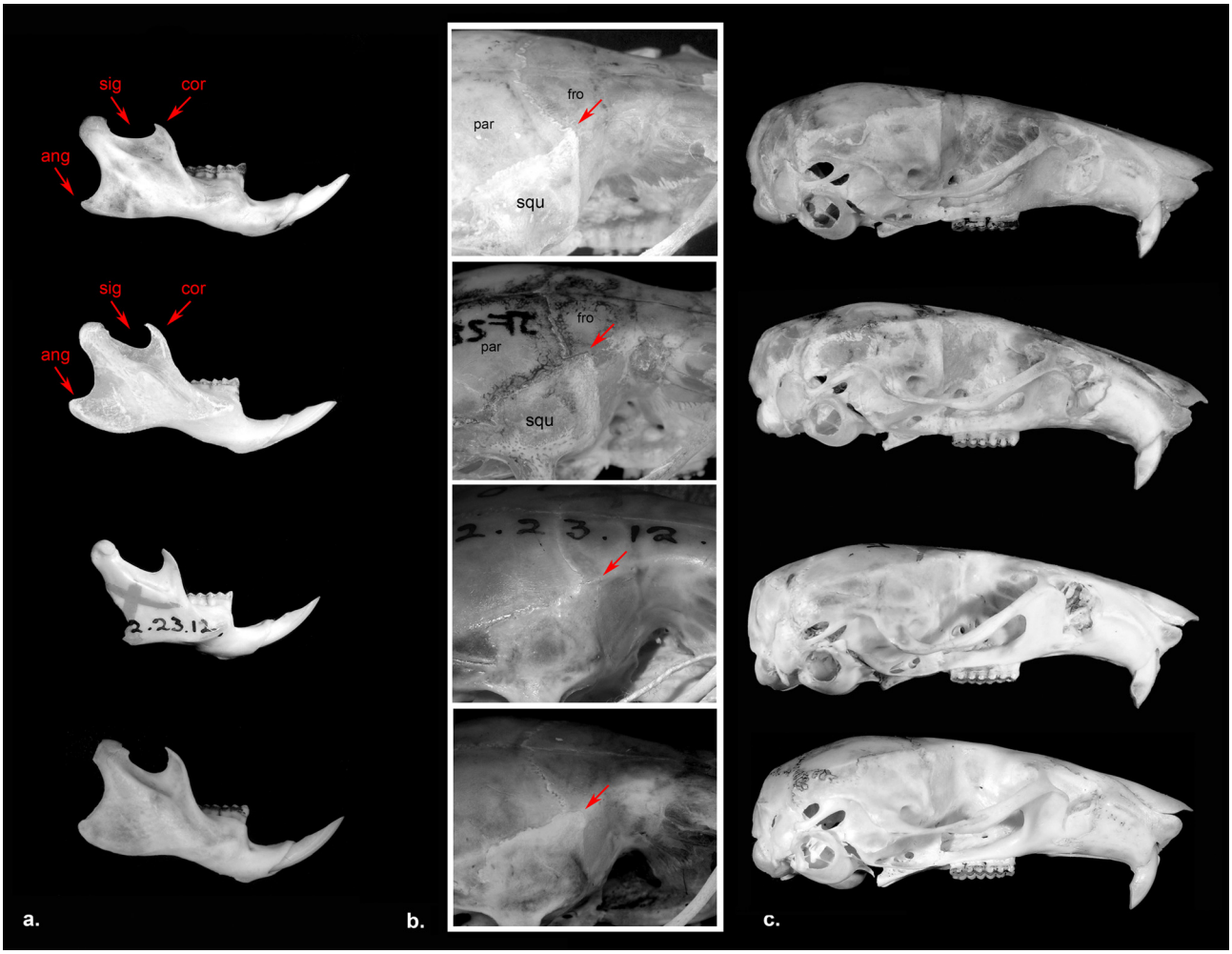

FIGURE 4. (a) Mandibles of (top to bottom) *Delomys* **sp. nov.** (MN69712, Campos do Itatiaia, Itatiaia, RJ, 2450m), *D. dorsalis* (MN78927, Maromba, Itatiaia, RJ, 1170m), the holotype of *D. dorsalis collinus* (BMNH14.2.23.12, Itatiaia, RJ, 1470m) and *D. sublineatus* (MN78674, Caucaia do Alto, SP, 930m). (b) Variation in the contact of the frontoparietal and frontosquamosal sutures of (top to bottom) *Delomys* **sp. nov.**, *D. dorsalis*, the holotype of *D. dorsalis collinus* and *D. sublineatus*. *Arrow* points to the anterodorsal limit of squamosal. (c) Lateral view of skulls of (top to bottom) *Delomys* **sp. nov.**, *D. dorsalis*, *D. dorsalis collinus* and *D. sublineatus* (MVZ183076, Estação Ecológica de Boracéia, SP, 935m). Abbreviations: *ang*—angular process, *cor*—coronoid process, *fro*—frontal, *par*—parietal, *sig*—sigmoid notch, *squ*—squamosal.

Other qualitative cranial characters related to the rostral region also vary among species, but in a less discrete manner. *Delomys sublineatus* (Fig. 5d) exhibits a relatively shorter and more blunted rostrum in relation to those of *Delomys* **sp. nov.** (Fig. 5a), *D. dorsalis* (Fig. 5b) and *D. d. collinus* (Fig. 5c) which, by contrast, exhibit elongated and terminally pointed rostra. The variation in rostral protrusion can be clearly noted by the anterior extension of the nasal tube (formed by the lateral fusion of the premaxillaries with the nasals) in relation to the gnathic process between the incisors, as seen in lateral view (Fig. 4c). In *Delomys sublineatus* the nasal tube terminates just anterior to the gnathic process, while in *Delomys* **sp. nov.**, *D. d. collinus* and *D. dorsalis* it projects well beyond the level of the gnathic process, terminating almost at the anteriormost end of the premaxilla.

External characters exhibit variation among *Delomys* species, as already recognized by Voss (1993), despite some degree of overlapping among *Delomys* **sp. nov.** and *D. dorsalis*, especially in fur length and color pattern. *Delomys dorsalis* and the holotype of *D. d. collinus* exhibit soft and dense dorsal fur, contrasting to the coarser dorsal pelage of *D. sublineatus,* as previously noted by Thomas (1917) in his description of *D. d. collinus*. *Delomys* **sp. nov.** tends to exhibit longer dorsal guard hairs along the middorsum in the cervical region, varying from 15 to 20 mm in length. Conversely, the series of *D. dorsalis* from Itatiaia (8 to 15 mm), as well as the holoype of *D. dorsalis collinus* (9–10 mm, measured in the holotype), tend to exhibit shorter hairs in this body region. Specimens of *Delomys sublineatus* have the shortest guard hairs among the three species, with its longest ones reaching 6–8 mm.

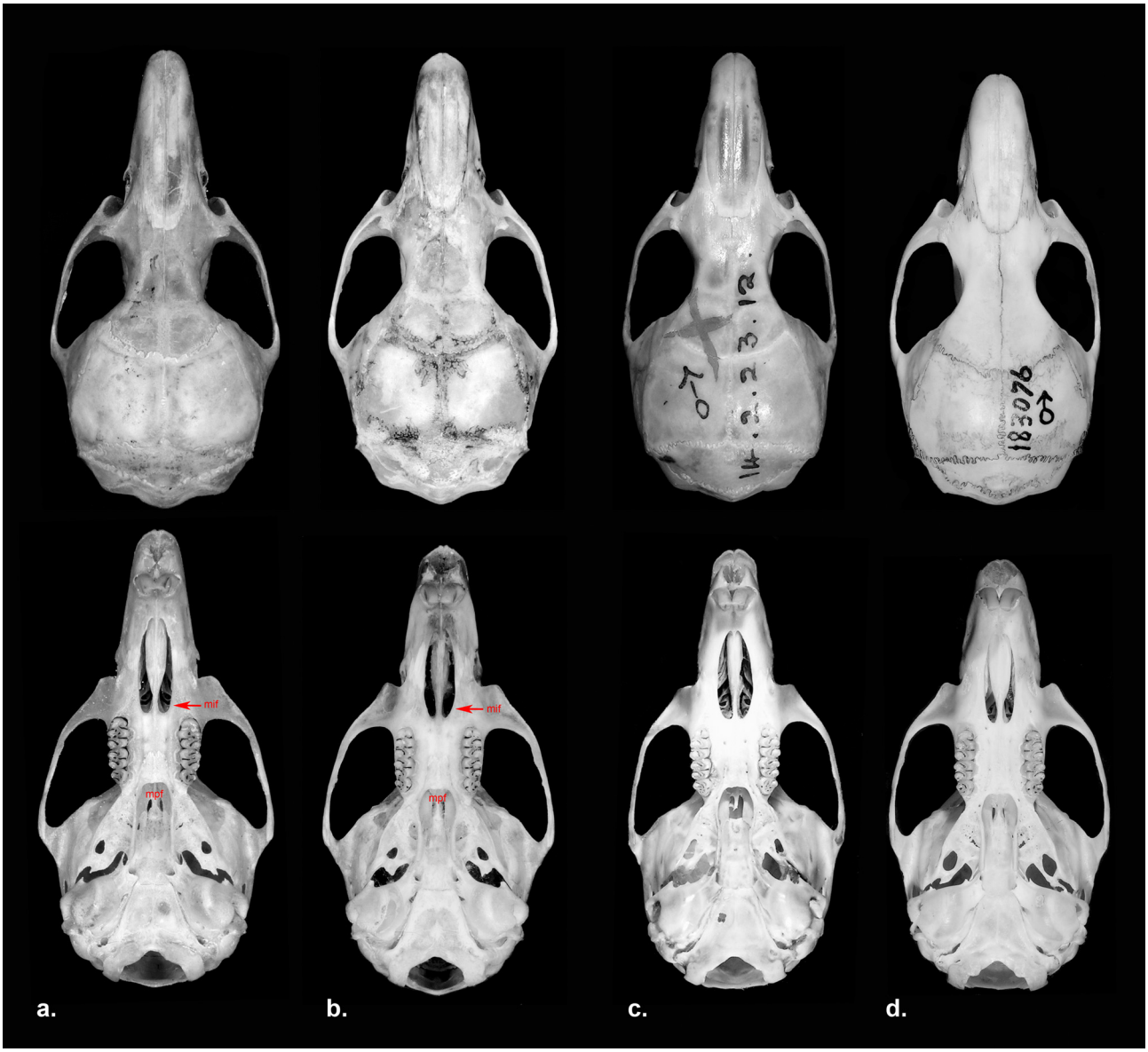

FIGURE 5. Dorsal and ventral views of skulls of (a) *Delomys* **sp. nov.** (MN69712, Campos do Itatiaia, Itatiaia, RJ, 2450m), (b) *D. dorsalis* (MN78927, Maromba, Itatiaia, RJ, 1170m), (c) *D. dorsalis collinus* (BMNH14.2.23.12, holotype, Itatiaia, RJ, 1470m) and *D. sublineatus* (MVZ183076, Estação Ecológica de Boracéia, SP, 935m). Abbreviations: *mif*—maxillary margin of incisive foramen, *mpf*—mesopterygoid fossa.

Adults of *Delomys* **sp. nov.**, *D. dorsalis* and the holotype *D. d. collinus* display a similar general dark-cinnamon general dorsum color, always darker than the condition seen in *D. sublineatus*, which has a predominantly cinnamon-yellow general dorsal color. Nevertheless, all species of *Delomys* tend to exhibit a darker mid-dorsum, sometimes delineated by a well-defined mid-dorsal stripe extending continuously from the nape to the tail base, a character frequently emphasized in descriptions of the genus. Despite this tendency, the three species vary in the extent to which this mid-dorsal stripe is well defined in relation to the adjacent fur. A mid-dorsal stripe is well noticeable and defined in 74% of the *D. dorsalis* specimens (illustrated by the *D. dorsalis* specimen of Fig. 6), while only 44% of the *D. sublineatus* specimens and 31% of the *Delomys* **sp. nov.** specimens exhibit well defined stripes. The holotype of *D. d. collinus* exhibits an ill-defined mid-dorsal stripe, which becomes more sparse in the scapular and head regions (Fig. 6). This condition is exhibited by specimens of both *D. dorsalis* (26%) and *Delomys* **sp. nov.** (74%, illustrated by the *Delomys* **sp. nov.** specimen in Fig. 6) even in sympatric samples, not allowing a complete discrimination among forms. Chromatic variation among the three species is also evident along the lateral fur, with *Delomys* **sp. nov.** generally exhibiting orangish tones along the body sides, while *D.*

dorsalis and the holotype *D. d. collinus* displays more brownish and relatively darker laterals (Fig. 6). *Delomys sublineatus* exhibits a brighter yellowish lateral color, with some yellow-banded hairs arranged as a narrow lateral line, marking a clear division between the lateral and ventral sides in most specimens. The dorsal surfaces of the hind feet and digits in the three species are covered by short whitish hairs, but in *Delomys* **sp. nov.**, *D. dorsalis* and the holotype of *D. d. collinus* some dorsal hairs on the hind feet have dark bases, especially on the central region of the pes, thus displaying a buffy or soiled general aspect, as already noted by Voss (1993) for *D. dorsalis*. *Delomys sublineatus*, on the other hand, lacks hairs with dark bases on the dorsal surface of pes, exhibiting more whitish hindfeet.

Tail color pattern varies significantly among the three species. All specimens of *Delomys* **sp. nov.** have tails that are bicolored along most of their length, displaying a markedly pale venter throughout their proximal two-thirds. By contrast, the holotype of *D. d. collinus* and all specimens of *D. dorsalis* from Itatiaia exhibit a weakly bicolored tail, with a pale venter restricted to the first proximal third of the tail length, a condition also remarked by Thomas (1917) in specimens of *D. d. collinus* (Fig. 6). The differences in tail color are consistent between sympatric samples of the two species from Itatiaia, but samples of *D. dorsalis* from Serra do Mar are polymorphic for this character. The tail color pattern of *D. sublineatus* is similar to that of *Delomys* **sp. nov.**, with the ventral coloration being slightly brighter or whitish throughout most of the tail length.

The tail-to-body length ratio (TL/HBL) varies among the species, with *D. sublineatus* generally displaying tails shorter than head-and-body length (ratio <1), as noted by Voss (1993). Nevertheless, the samples at hand have overlapping ranges for this ratio (*Delomys* **sp. nov.** from Itatiaia: 0.70–1.15; *D. dorsalis* from Mantiqueira clade: 0.71–1.37; *D. sublineatus*: 0.54–1.00), hampering the use of this character to discriminate the three species. The holotype of *D. d. collinus* has a tail that is slightly longer (132 mm) than its head-and-body length (130 mm), displaying a ratio of 1.01 and falling within the variation interval of both *Delomys* **sp. nov.** and *D. dorsalis*.

Female mammae number is also variable in the genus as initially acknowledged by Thomas (1917), who remarked that the only female of *D. dorsalis collinus* from Itatiaia examined by him exhibited six mammae (because the pectoral pair was absent), while *D. dorsalis dorsalis* samples from southern Brazil (Paraná and Rio Grande do Sul states) exhibited eight mammae (pectoral pair present). Later, Voss (1993) corroborated this geographic variation pattern and considered the absence of a pectoral pair of mammae as the sole basis for recognition of *D. dorsalis collinus*. The inspection of this character in the few lactating females of *Delomys* **sp. nov.** (n = 2) and *D. dorsalis* (n = 5) available from Itatiaia reveals that the pectoral pair is lacking in both species, thus, not being useful to distinguish them in sympatry. On the other hand, the presence of a pectoral pair of mammary glands does in fact vary geographically within *D. dorsalis* (see its species account below). All lactating females of *Delomys sublineatus* examined (n = 20) displayed eight mammae.

The general pentalophodont architecture of the molar enamel flexi and lophs is conservative among the three species of the genus, but there is relevant variation between *Delomys* **sp. nov.** and *D. dorsalis* specimens from Itatiaia in molar general size and in the procingula structures of upper and lower M1 of adults with slightly worn teeth. In *Delomys* **sp. nov.** the anterocone of M1 is more asymmetrically divided than in *D. dorsalis* from Itatiaia, with the anteromedian flexus penetrating the procingulum at a point more lingually displaced in relation to the labial limit of the protoflexus, resulting in a much smaller anterolingual conule (Fig. 7a). On the other hand, in *D. dorsalis* the anteromedian flexus penetrates the procingulum at the same level of the labial limit of the protoflexus, providing a comparatively less asymmetrical aspect to the anterolingual and anterolabial conules (Fig. 7b). The molars of the holotype of *D. d. collinus* are moderately worn and some internal structures are not clearly discernible anymore. Nevertheless, the asymmetry level between the labial and lingual M1 anteroconules resembles more the condition seen in *D. dorsalis* from Itatiaia (Fig. 7c). The lower m1 of *Delomys* **sp. nov.** also exhibits a deeper protoflexid and a more elongated and diagonally oriented protolophid, which projects to the level of metaconid margin (Fig. 7d), contrasting with the shallower protoflexid and relatively reduced and more transversally projected protolophid of *D. dorsalis* (Fig. 7e). The lower molars of the holotype of *D. d. collinus* are too worn and the protolophid is not clearly discernible.

In summary, among the 15 qualitative morphological characters that vary among nominal taxa of *Delomys*, eight have fixed conditions in *Delomys* **sp. nov.** that distinguish it from *D. d. collinus*, *D. dorsalis* and *D. sublineatus* (Table 3). Among these distinctive characters, four are consistently divergent between *Delomys* **sp. nov.** and all samples of *D. dorsalis* (characters 2, 3, 4 and 5 in Table 3), and two are exclusively shared by *D. d. collinus* and *D. dorsalis* from Itatiaia (characters 3 and 14 in Table 3). By contrast, no traits are exclusively shared

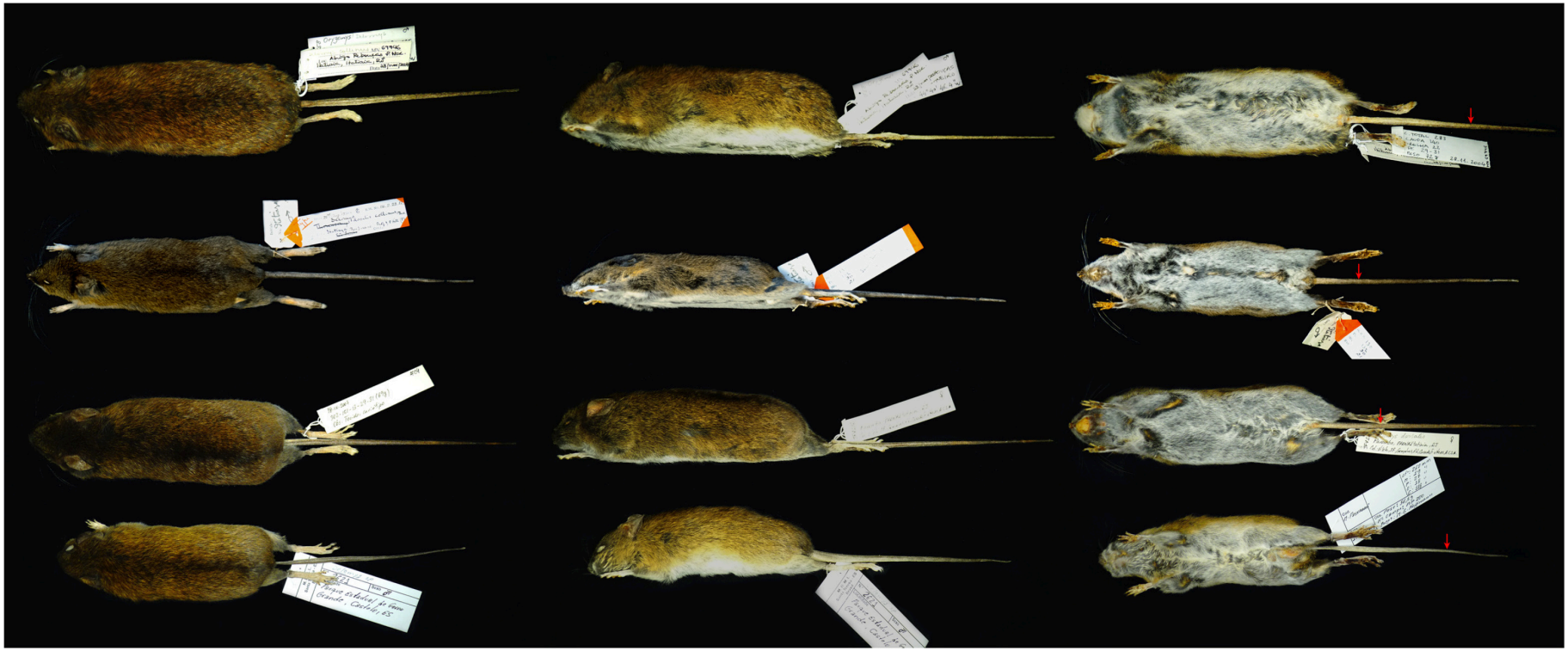

FIGURE 6. Dorsal, lateral and ventral views of skins of (top to bottom) *Delomys* **sp. nov.** (MN69746, holotype, Campos do Itatiaia, Itatiaia, RJ, 2450m), *D. dorsalis collinus* (BMNH14.2.23.12, holotype, Itatiaia, RJ, 1470m), *D. dorsalis* (MN78927, Maromba, Itatiaia, RJ, 1170m), and *D. sublineatus* (MBML2621, Parque Estadual de Forno Grande, Castelo, ES, 1200m). Arrows mark the posterior extent of the pale patch on tail venter.

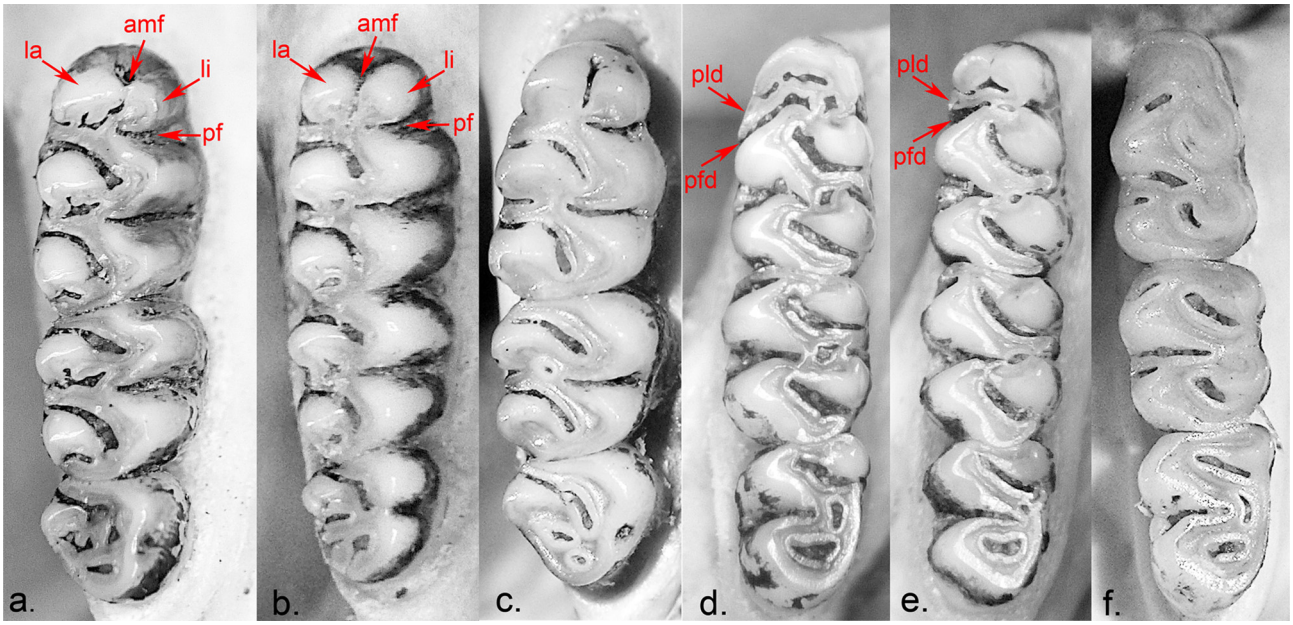

FIGURE 7. (a–c) Upper and (d–f) lower molar rows of *D. altimontanus* (MN69712, Campos do Itatiaia, Itatiaia, RJ, 2450m), *D. dorsalis* (MN60572, Brejo da Lapa, Itamonte, MG, 1843m) and the holotype of *D. dorsalis collinus* (BMNH14.2.23.12, Itatiaia, RJ, 1470m). Abbreviations: *amf*—anteromedian flexus, *la*—anterolabial conule, *li*—anterolingual conule, *pf*—protoflexus, *pfd*—protoflexid, *pld*—protolophid.

by *Delomys* **sp. nov.** and *D. d. collinus*. Therefore, the morphological evidence at hand suggests that the holotype of *D. d. collinus* is more closely associated with samples of *D. dorsalis* (with 2n=82/FN=80) than with samples of *Delomys* **sp. nov.** (with 2n=82/FN=86).

Quantitative characters. Patterns of craniodental morphometric variation among the three species were assessed quantitatively by means of Canonical Variate analyses (CVA) based on 14 craniodental measurements taken from 308 intact adult specimens representing the 32 populations included in the molecular phylogenetic analyses (Table 1). The three species previously recognized are recovered as three narrowly overlapping clusters dispersed along the first canonical variate (CV1), with *Delomys* **sp. nov.** also departing from both *D. dorsalis* and *D. sublineatus* along the second canonical variate (CV2) (Fig. 8a). In this ordination, CV1 accounts for 86.8% of the among-species variation while the CV2 accounts for 13.2% of this variation. Most craniometric characters are positively correlated with CV1, but vary in their vector correlations along CV2 (Fig. 8b). *Delomys* **sp. nov.** represents an extreme along the CV1 axis, differing from both *D. dorsalis* and *D. sublineatus* by relatively larger values for most cranial characters, especially those related to the rostral component of the skull (LD, LIF). *Delomys sublineatus* marks the opposite extreme of size variation along CV1, exhibiting shorter rostra and overall smaller crania in relation to the other two species. The second canonical variate provides further evidence for the discrimination of *Delomys* **sp. nov.** in relation to *D. dorsalis,* due to relatively wider molars (BM1), longer palatal bridges (LPB), narrower interorbits (LIB) and flattened braincases (DB). The discriminant functions correctly classified 95.4% of specimens of *Delomys* **sp. nov.**, and respectively 85.9% and 93.8% of the *D. sublineatus* and the *D. dorsalis* individuals. However, when only sympatric samples of *Delomys* **sp. nov.** and *D. dorsalis* from Itatiaia are highlighted in the multivariate space, the discrimination between these two species becomes clearer, with all specimens being correctly classified to the two samples (Fig. 8c). The pattern of discrimination between these two species was further validated in a bivariate plot combining the Length of upper molars (LM) and the Breadth of M1 (BM1), where the Itatiaia specimens of *Delomys* **sp. nov.** are slightly differentiated from those of *D. dorsalis* by the combination of longer and wider molars.

The discriminant functions were also used to calculate scores for the holotype of *D. dorsalis collinus* allowing its *a posteriori* interpolation in relation to the Itatiaia samples of *D. dorsalis* and *Delomys* **sp. nov.** The placement of the holotype of *D. d. collinus* reveals that it has greater similarities to the Itatiaia sample of *D. dorsalis* than to the sympatric sample of *Delomys* **sp. nov.**, despite having intermediate CV1 and CV2 scores (Fig. 8c). The dental measurements of the holotype of *D. d. collinus* also favor its allocation to the Itatiaia sample of *D. dorsalis*,

differing from all sympatric *Delomys* **sp. nov.** specimens by exhibiting shorter and narrower upper molars (Fig. 8d). Nevertheless, since the craniometric distinction between *Delomys* **sp. nov.** and *D. dorsalis* is subtle, the dental measurements do not provide an unequivocal allocation of the holotype of *D. d. collinus* within the samples of *D. dorsalis* from the Itatiaia mountain range. Altogether, the best morphological evidence for the distinction of *Delomys* **sp. nov.** and allocation of *D. d. collinus* to *D. dorsalis* come from the comparisons of qualitative characters discussed previously and summarized in Table 3. Based on these results, we provide the description of the new form and an updated account of *Delomys dorsalis*.

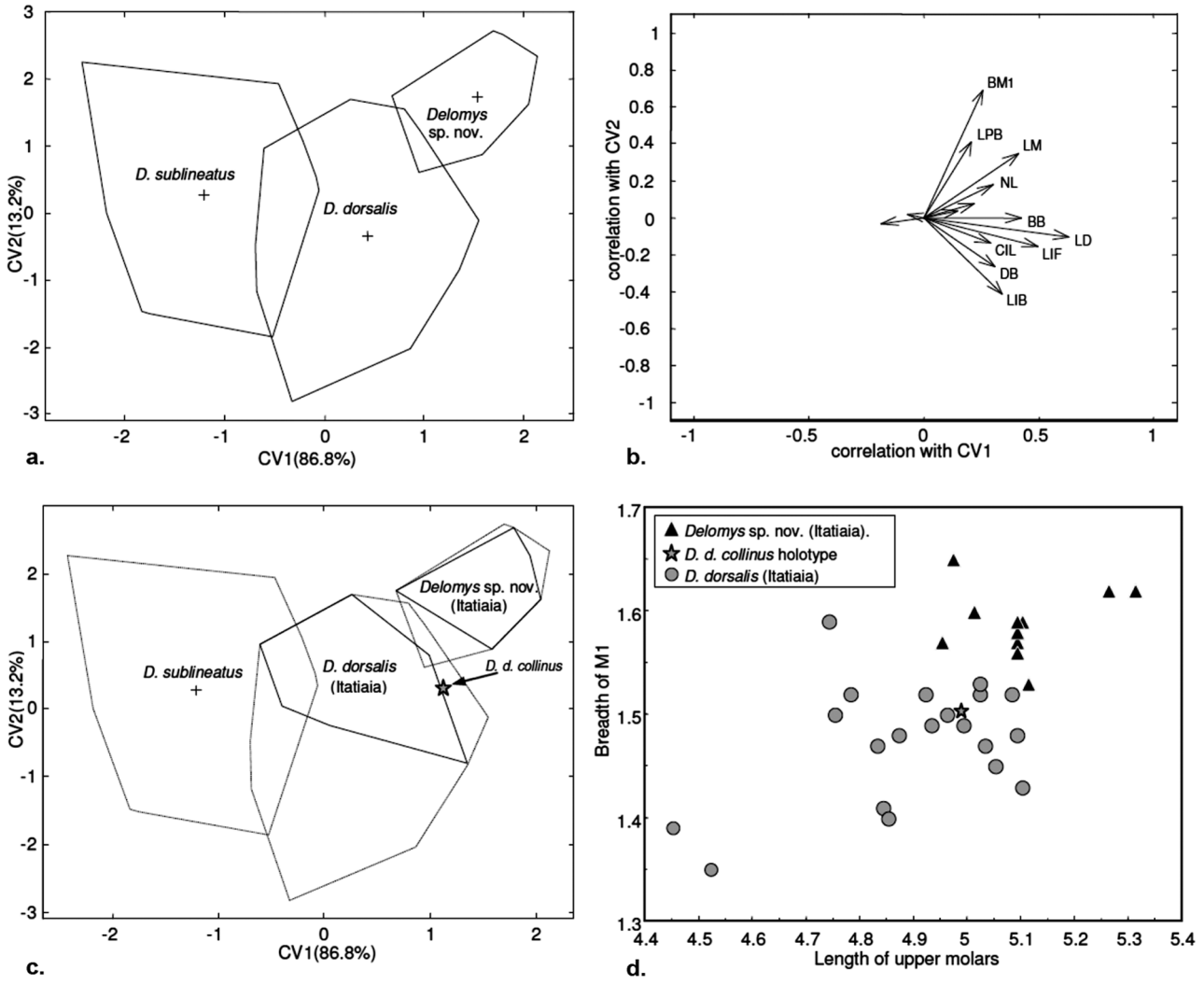

FIGURE 8. Craniometric discrimination among species of *Delomys:* (a) CVA analysis among samples with karyotypic and/or molecular data, and (b) respective vector correlations among characters and CVA axes. (c) CVA analysis with sympatric samples of *Delomys* **sp. nov.** and *D. dorsalis* from Itatiaia Mt. highlighted, showing the allocation of the *D. d. collinus* holotype. (d) Bivariate plot of most discriminant craniometric characters to discriminate between *Delomys* **sp. nov.** and *D. dorsalis* with the measurements of *D. d. collinus* holotype included.

Systematics

Delomys altimontanus, new species

Delomys collinus: Bonvicino & Geise 1995 (not *collinus* Thomas 1917)
Delomys dorsalis: Hershkovitz 1998 (not *dorsalis* Hensel 1972)
Delomys sublineatus: Hershkovitz 1998 (not *sublineatus* Thomas 1903)

Type material. The holotype, MN69746, is an adult male collected by Pablo R. Gonçalves, João A. Oliveira,

Cibele R. Bonvicino and Maria Olímpia G. Lopes on 28 November 2004 (field number JAO 1558). The specimen was collected in a Sherman™ trap placed in a montane shrub dominated by bamboo at the margin of the Campo Belo stream, close to the Abrigo Rebouças. The specimen consists of a skin, skull and postcranial skeleton accompanied by a liver tissue sample preserved in ethanol and femoral medullar cells preserved in methanol/acetic acid solution. We designate as paratypes seven specimens collected in the localities of Abrigo Rebouças (MN69712, male) at Itatiaia -, Rio de Janeiro state, and Brejo da Lapa (MN60573-60576**,** 60584, 60585), municipality of Itamonte, Minas Gerais state.

Type locality. Campos do Itatiaia, (22°23'26"S, 44°40'14"W, 2450m altitude), near Abrigo Rebouças, Parque Nacional do Itatiaia, municipality of Itatiaia, Rio de Janeiro state, Brazil (locality 21, Figs. 1 and 12a).

Etymology. The specific epithet *altimontanus* refers to the restricted altitudinal distribution of the species, exclusively inhabiting the forested altiplano of the Mantiqueira mountain range in southeastern Brazil (from the Latin *altus* = high + *montanus* = mountain inhabitant).

Distribution. This species exhibits a disjunct distribution with reported populations apparently restricted to the highest altitudinal forested zones of 1800 to 2500 m in the Itatiaia and Caparaó mountain ranges, which are two different offshoots of the Mantiqueira mountain complex. Populations of *Delomys* that have been sampled in the intervening mountain chains that are part of the coastal Serra do Mar mountain complex, such as the Serra da Bocaina, Serra dos Órgãos and Serra do Desengano (in Rio de Janeiro state), or even in lower mountains of the Mantiqueira complex (Serra do Brigadeiro in Minas Gerais state), have been identified as either *D. dorsalis* or *D. sublineatus* (Delciellos *et al.* 2012; Modesto *et al.* 2008; Moreira *et al.* 2009; Olifiers *et al.* 2007). These facts suggest that the current disjunct distribution of *Delomys altimontanus* **sp. nov.** is a relict of a formerly wider distribution rather than a sampling artifact across Southeastern Brazil.

It is probable that additional populations of *D. altimontanus* occur throughout the Mantiqueira range, especially in the mountains adjacent to Itatiaia that extend to the southwestern into São Paulo state (Campos do Jordão, Piquete) and Minas Gerais (e.g., Itamonte, Delfim Moreira, Passa Quatro). Nevertheless, available samples from these localities do not show the diagnostic morphological or genetic characters of *D. altimontanus*, rather representing *D. dorsalis* populations.

Karyotype. The karyotype of *Delomys altimontanus* (Fig. 9) exhibits 2n = 82 and FN=86, with an autosomal complement constituted by 3 pairs of biarmed chromosomes, 27 pairs of acrocentrics, a large-sized submetacentric X chromosome and a small metacentric Y chromosome, as previously described by Bonvicino & Geise (1995). *Delomys altimontanus* diverges from *D. sublineatus* (2n=72, FN=90) in both diploid and fundamental numbers, but shares the same diploid number with *D. dorsalis* (2n=82), from which it can be distinguished by the morphology of three small-sized biarmed pairs of autosomes. This karyological difference between *Delomys altimontanus* and *D. dorsalis* probably evolved through pericentric inversions involving the smallest pairs of autosomes.

Diagnosis. A medium-sized species of the genus *Delomys* with soft and long dorsal pelage, predominantly cinnamon-brown grizzled with yellow, but becoming brighter orange along the flanks; tail as long as head-and-body length and strongly bicolor throughout most of its length; skull with pronounced rostrum and elongated nasal tube projecting beyond the gnathic process; relatively longer and wider molar series than in other congeneric taxa; relatively narrow interorbit; supraorbital region exhibiting the fronto-parietal (coronal) suture collinear with the fronto-squamosal suture, without an area of dorsal contact between squamosal and frontal; incisive foramina with straight margins along the maxillary; mesopterygoid fossa equally wide at its anterior and posterior portions; mandible with wide, shallow and symmetrically excavated sigmoid notch, delicate coronoid process and reduced angular process; karyotype with 2n=82 and FN=86.

Description. Body pelage soft, dense and long, with guard hairs along the cervical region of the dorsum varying in length from 15 to 20 mm. General dorsal color is cinnamon-brown in adults, brighter and orangish along the laterals and gradually darker towards the mid-dorsum, generally forming a ill-defined median stripe in most specimens, which extends from the nape to the base of tail (Fig. 10). In old adults the sides of body are more rusty colored due to the presence of bright orange bands on hairs, while young specimens generally display a duller and grayer dorsal and lateral color with few traces of yellowish tone. Ventral pelage predominantly white, covered by whitish hairs with wide dark-gray bases frequently showing through. Head similar in coloration to the mid-dorsum, becoming brighter at the cheeks. Neck and chin region covered by smaller bicolored hairs, similar in coloration to those of the ventral region. Eyes large and surrounded by short dark hairs, forming a narrow eye-ring. Mystacial, superciliary, genal, submental, interramal and carpal vibrissae present. Mystacial vibrissae long, with the two

longest reaching the distal tip of the pinnae when laid back. Pinnae large (Table 4) and sparsely covered with short hairs on its internal surface, but more densely furred on its dorsal surface.

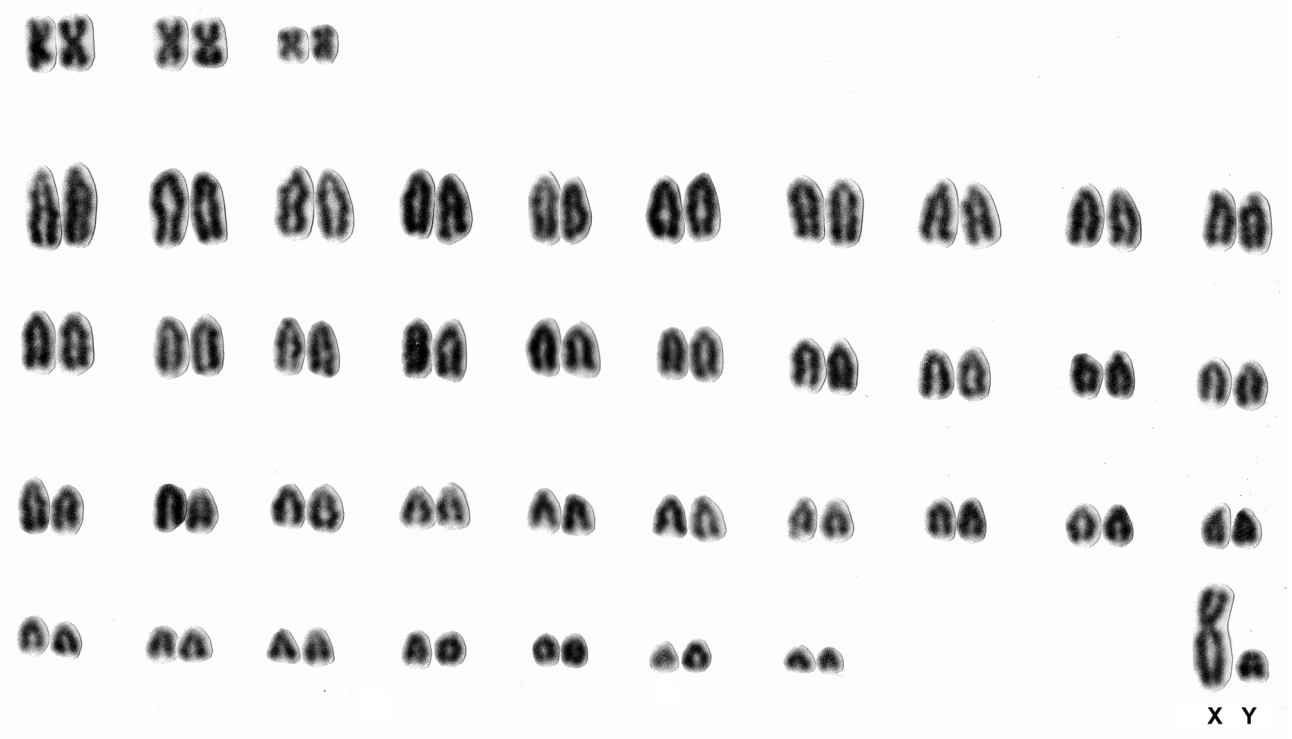

FIGURE 9. Karyotype of *D. altimontanus* from Campos do Itatiaia, Itatiaia, RJ, 2450m (MN 69712, male) in conventional staining

Cheiridia dorsally covered by short whitish hairs, most of them with dark bases, specially at the proximal metacarpal and metatarsal regions, giving a general soiled or gray aspect to the dorsal surfaces of manus and pes. Hindfoot long and narrow. Ungual tufts long and conspicuous, completely enclosing the claws on digits I–IV, but reduced or vestigial on digit V. Middle digits (II–IV) are longer than the outer digits (I and V), with digit III slightly longer than digits II and IV. Digit I is longer than digit V, with its claw extending to the middle of the first phalange of digit II, while the claw of digit V reaches the first interphalangeal joint of digit IV. Plantar surface naked over the heel and much of the metatarsal region, being more squamate over the digits surface. Six fleshy plantar pads present (hypothenar, thenar and four interdigital pads).

Tail slightly longer to, or as long as, the head and body length (Table 4), sparsely covered by short hairs, and displaying a bicolor pattern throughout more than half of its length. The tail color is predominantly dark brown throughout its entire dorsum, but markedly whitish to buffy in the venter, throughout its first two proximal thirds, gradually intergrading to dark-brown towards the distal third. The brighter ventral color of the tail is provided by entirely whitish short hairs, which in the base of the tail span two to three scales in length. Towards the tail dorsum and the distal third of the tail venter, hairs with wide dark brown basal bands become more common, providing darker tones.

Six mammae present in lactating females, distributed in inguinal, abdominal and postaxial pairs (pectoral pair lacking), displaying the mammary formula of 0/2/2/2.

Cranium large and wide (CIL = 31.4–27mm, BB = 12.73–11.7mm, Table 4), with a narrow and elongated rostrum, biconcave and narrow interorbit and globular braincase with smooth edges (Fig. 11). Nasals long (NL = 14.65–11.75mm) and narrow, extending posteriorly beyond the fronto-premaxillary suture. The nasals taper more abruptly at their anterior midlength and then more subtly before converging at the fronto-nasal suture. Lacrimals squared and relatively large, contacting both the frontal and maxillary bones. Interorbital region relatively narrow and biconcave, exhibiting the typical "hourglass" morphology (Voss 1993) with smooth edges and without supraorbital crested margins, even in older adults. Fronto-nasal suture slightly depressed, with frontal sinuses dorsally prominent. Fronto-parietal (=coronal) suture U-shaped, generally open angled in most specimens, but also

TABLE 4. External and cranial measurements of adult specimens from populations and intraspecific clades of *Delomys altimontanus*, *D. dorsalis* and *D. sublineatus*. Sample statistics include sample size (*n*), mean and standard deviation (mean±standard deviation).

	***D. altimontanus* (*n*=22)**		***D. dorsalis* (*n*=191)**					***D. sublineatus* (*n*=97)**	
Characters	Caparaó (*n*=11)	Itatiaia (*n*=11)	*collinus* holotype	Mantiqueira clade (*n*=23)	Serra do Mar clade (*n*=83)	Southern clade (*n*=80)	topotypes (*n*=4)		Holotype
HBL	134±12	130±9	130	125±9	129±13	126±14	–	128±11	148
TL	123±14	126±14	132	128±10	130±14	136±11	–	106±13	120
HF	31±2	32±1	30	31±2	31±1	29±2	–	29±2	30
EL	20±1	22±1	21	22±1	21±2	21±2	–	21±2	21
CIL	29.87±0.89	29.66±1.25	29.33	29.08±0.97	30.15±2.07	29.53±2.00	28.52±0.97	28.73±1.46	–
NL	13.99±0.45	13.62±0.67	12.83	13.18±0.63	13.30±0.83	13.28±0.86	13.35±0.53	12.95±0.75	13
LD	9.23±0.30	8.93±0.55	8.68	8.72±0.39	8.86±0.57	8.80±0.51	8.70±0.25	8.17±0.46	9.2
LPB	5.34±0.28	5.40±0.23	5.11	5.30±0.29	5.02±0.30	5.04±0.26	4.98±0.23	5.03±0.28	5.24
LM	4.99±0.12	5.10±0.11	4.98	4.89±0.18	4.91±0.15	4.70±0.16	4.51±0.26	4.72±0.18	4.72
BM1	1.58±0.04	1.59±0.03	1.5	1.47±0.05	1.49±0.06	1.45±0.06	1.37±0.05	1.47±0.07	1.5
LIF	6.77±0.19	6.98±0.44	6.47	6.57±0.36	7.00±0.41	6.65±0.43	6.25±0.04	6.36±0.35	7.02
BR	6.08±0.30	6.07±0.30	5.94	6.12±0.34	6.15±0.29	6.03±0.36	5.78±0.13	6.13±0.32	6.61
DR	6.30±0.22	6.15±0.33	6.2	6.18±0.31	6.47±0.37	6.23±0.36	5.94±0.30	6.43±0.35	6.89
BPB	3.48±0.17	3.30±0.20	3.49	3.34±0.18	3.33±0.21	3.33±0.27	3.12±0.42	3.28±0.24	3.12
BZP	2.98±0.17	3.05±0.17	3.03	3.04±0.19	2.97±0.22	2.87±0.24	2.76±0.38	2.86±0.21	3
LIB	5.21±0.11	5.18±0.18	5.32	5.11±0.16	5.44±0.20	5.23±0.18	5.14±0.14	5.12±0.22	5.25
BB	12.43±0.23	12.85±0.40	13.79	12.34±0.42	12.38±0.43	12.37±0.45	12.55±0.59	11.97±0.73	–
DB	8.91±0.34	8.99±0.39	9.07	8.95±0.32	9.17±0.30	8.90±0.28	8.94±0.26	8.80±0.33	–

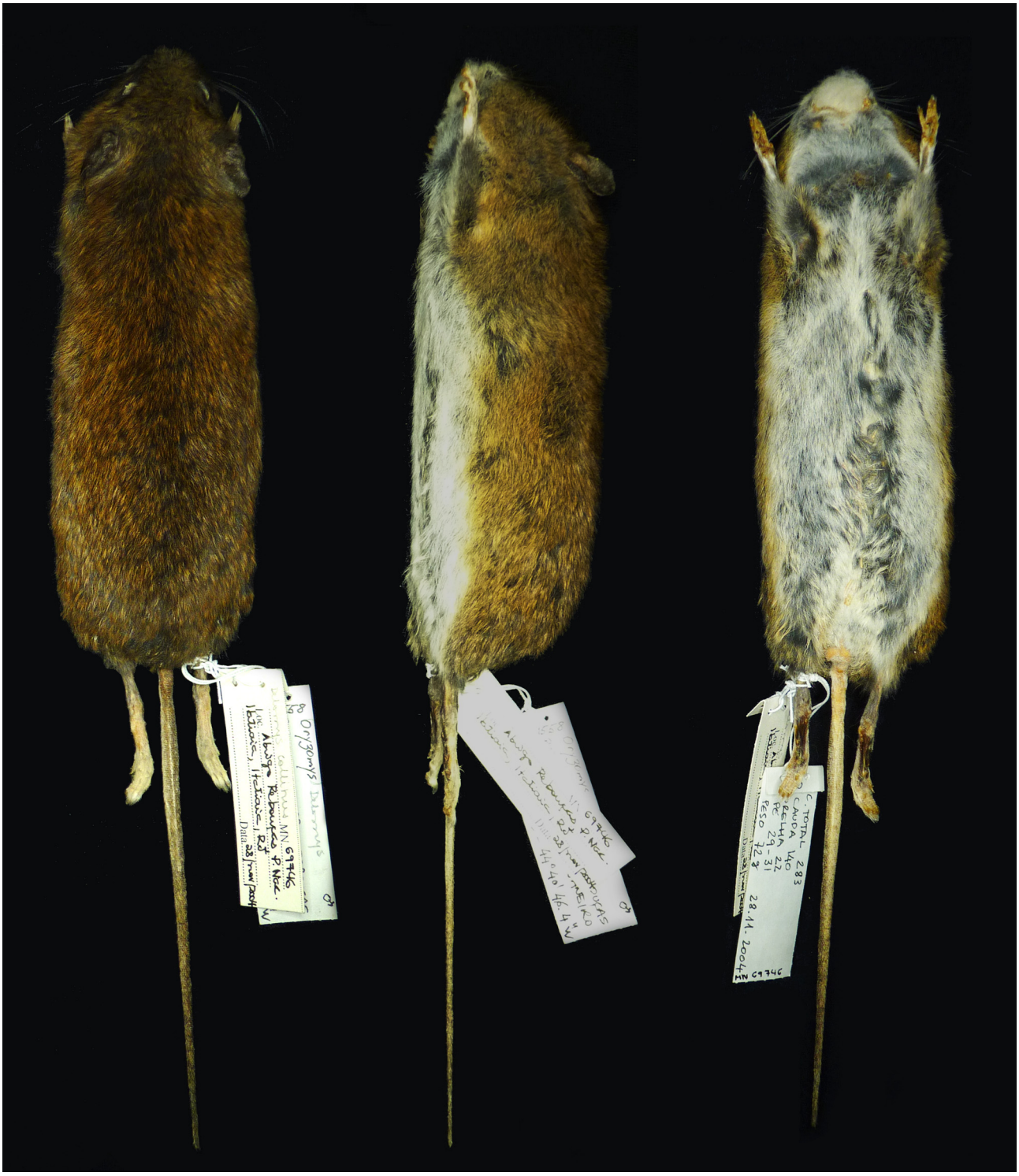

FIGURE 10. Dorsal, lateral and ventral views of the skin of the holotype of *D. altimontanus* from Campos do Itatiaia, Itatiaia, RJ, 2450m (MN 69746, male).

sharply angled in some older adults, especially towards its lateral limits. Fronto-parietal and fronto-squamosal sutures collinear, as both the parietal and squamosal bones contact the frontal nearly at the same level along the postorbital wall, leaving no area for a contact between the squamosal and the dorsal surface of the frontal. Parietals wide and slightly expanded onto the lateral surface of the braincase near the squamosal root of the zygomatic arch. Interparietal moderately wide and semicircular, not contacting the squamosal laterally. Zygomatic plate broad and projected anteriorly to the base of the lacrimal capsule, forming a conspicuous zygomatic notch; its anterodorsal margin smoothly rounded. Posterior margin of the zygomatic plate situated anterior to the alveolus of M1.

Zygomatic arch laterally expanded, formed by a large jugal and non-overlapping maxillary and squamosal branches. Postorbital wall with small ridges near the squamosal root of the zygomatic arch, and a conspicuous buccinator-masticatory trough. Incisive foramina wide, with an inflated and expanded palatine process and reduced maxillary septum; lateral outlines of the incisive foramina are straight lined along their maxillary portions, being sharply bent only at their caudal ends, where they terminate anterior to the M1 alveolus. Palate surface flat, without expressive lateral troughs or posterolateral pits. Bony palate short, with the mesopterygoid fossa extending anteriorly between the molar rows; anterior margin of the mesopterygoid fossa biconcave in most specimens due to the presence of a sharp median process, but flat in a few specimens lacking this process, being equally wide at its anterior (near the level of sphenopalatine vacuities) and caudal portions (along the pterygoid processes) in specimens with intact pterygoids. Parapterygoid fossae shallow, at about the same level as the palate. Sphenopalatine vacuities reduced to narrow slits restricted to the presphenoid or completely ossified in a few specimens. Posterior opening of the alisphenoid canal and stapedial foramen large, sphenofrontal foramen and alisphenoid-squamosal groove conspicuous, conforming to the primitive carotid circulation pattern (Weksler 2006) or pattern 1 of Voss (1988). Alisphenoid strut absent, and buccinator-masticatory and accessory oval foramina confluent. Hamular process slender, delimiting a larger subsquamosal fenestra and smaller postglenoid foramen. Tegmen tympani present and connected to the posterior suspensory process of squamosal. Bullae globular, constituted by a large ectotympanic, which contributes to the wall of the carotid canal and restricts the exposed ventral surface of the periotic to a narrow lip. Mastoid completely ossified or with a narrow perforation on its posterodorsal limit.

Mandible high and without conspicuous masseteric crests (Fig. 11). Capsular process of lower incisive alveolus reduced to a slight elevation. Sigmoid notch wide, shallow and symmetrically incised; coronoid process reduced, not projecting beyond the dorsal limit of the condyloid process; coronoid and condyloid process connected by an elevated bony ridge that has about the same height as the coronoid process. Angular process reduced and not projected posteriorly beyond the limit of the condyloid process.

Incisors ungrooved, with yellow enamel bands. Upper incisors strongly opisthodont. Molars pentalophodont. Upper molar rows parallel sided, long (LM = 4.53–5.2 mm) and wide (BM1 = 1.34–1.64 mm) (Table 4). M1 with anterocone very asymmetrically divided by an anteromedian flexus, which penetrates the anterior margin of the procingulum at a point more lingually displaced in relation to the labial limit of the protoflexus, resulting in a much narrower anterolingual conule and a much wider anterolabial conule (Fig. 7a). Anteroloph well developed and connected to the anterolabial conule in worn molars, forming an anterofossete which is confluent with the anteromedian flexus. Paraflexus and metaflexus deeply incised into the occlusal surface, penetrating beyond the medial limit of the protoflexus and hypoflexus. Median mure connected to the protocone. Mesoloph well developed, stemming from the median mure and reaching the labial cingulum. Paracone with a reduced paralophule contacting the mesoloph in older adults and delimiting a large medial enamel fossete and a shallow mesoflexus in older adults. Posteroflexus conspicuous, but frequently reduced to an enamel island in most adults or completely lost in older individuals. M2 squared and with narrow anteroloph and shallow protoflexus. M2 mesoloph as developed as in M1, also contacting the paralophule and delimiting a large medial enamel fossete. Median mure similar to that of M1. M3 small and triangular, with deep paraflexus and narrow anteroloph present. Mesoflexus and metaflexus reduced to enamel islands in adult individuals. Mesoloph present, but fully coalesced to the paracone at the labial margin. Hypocone reduced and hypoflexus shallow. Metacone, posteroloph and posteroflexus not identifiable in adult specimens.

Lower molar series longer and narrower than the upper series (length = 5.3–5.47 mm; width of m1 = 1.24–1.36 mm). Procingulum of m1 narrow, with anteroconid asymmetrically divided by a shallow anteromedian flexid (Fig. 7d); anteromedian fossetid wide and fused to anteromedian flexid in younger individuals; anterolophid absent; protolophid well developed and diagonally projected to the labial margin, contacting the anterolabial conulid at its medial portion; protoflexid deeply incised into the occlusal surface; metaflexid subdivided into a shallow lingual fold and a small enamel island, which is separated from the protoflexid by the anterior murid; mesolophid well developed and projected lingually, isolated from the metaconid by a deep mesoflexid and connected to the entoconid by a lophulid; ectostylid present and well developed in most specimens, and in older adults resembling an ectolophid; posteroflexid deep and posterolophid wide; m2 similar to m1, with a variably present ectolophid; reduced anterolabial cingulum and shallow protoflexid as sole remnant structures of the procingulum; m3 about the same size as m2; anterolabial cingulum and protoflexid absent; mesolophid barely distinguishable in adult molars; entoflexid and posteroflexid as enamel islands; hypoflexid deep; ectostylid reduced and ectolophid usually absent.

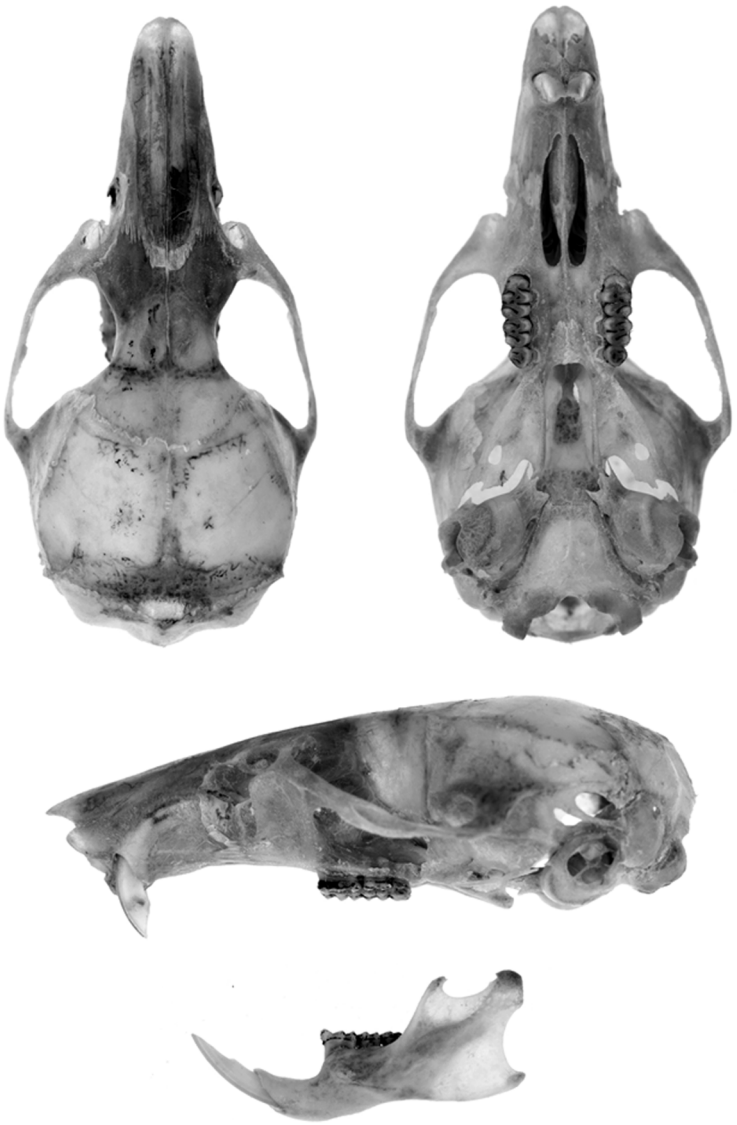

FIGURE 11. Dorsal, ventral and lateral views of the skull of a specimen of *D. altimontanus* from Campos do Itatiaia, Itatiaia, RJ, 2450m (MN 69712, male).

Variation in *Delomys altimontanus*. Nine *cytb* haplotypes were identified among the 15 sequenced *D. altimontanus* specimens from Caparaó Mt. (locality 6) and from two high-elevation localities in Itatiaia (localities 18 and 21) (Fig. 12a). The genealogical relationships portrayed by the statistical parsimony network do not support the haplotypes from Itatiaia and Caparaó as two exclusive genetic groups, in spite of the large distributional gap (ca. 300 km) between these two populations (Fig. 12b). Haplotype 8 from Caparaó, for instance, is connected to haplotype 3 from Itatiaia by three mutational steps rather than to the other two most frequent haplotypes from Caparaó (haplotypes 1 and 7), from which it differs by eight mutational steps. The six Itatiaia haplotypes are positioned in the center of the network, differing from one another by just a few mutational steps (one to six). The most frequent of these haplotypes (haplotype 4) is shared between two adjacent collecting sites (localities 18 and 21, Fig. 12b). The quantitative results of the AMOVA analysis show that most variation among haplotypes (69.3%) is due to differentiation within populations or within collecting localities rather than among the two disjunct populations (30.7%). Fixation indexes are also not statistically different from zero (Φ_{SC}= 0.4861, p=0.1212; Φ_{CT}= 0.3069, p=0.3118), suggesting a low level of geographic differentiation in *D. altimontanus*.

Despite the low level of geographic structure suggested by molecular variation in *D. altimontanus*, a Canonical Variates analysis of craniometric characters revealed that the Caparaó population differs from Itatiaia by having a somewhat longer rostrum (LD) and wider interorbit (LIB), whereas the Itatiaia population has slightly wider

molars (BM1) and longer incisive foramina (LIF) (Fig. 12c). All specimens from Caparaó could be correctly reclassified into their respective group, while 91.7% of the specimens from Itatiaia were correctly reallocated by minimum Mahalanobis distances. However, a bivariate plot combining the incisive foramina and diastema lengths shows that the segregation between the two samples is much more subtle, with at least four specimens completely overlapped (Fig. 12d). The dorsal pelage of Caparaó specimens also tend to be more orangish along the flanks than in Itatiaia specimens. Nevertheless, the Caparaó sample we examined has a larger number of old adult individuals. Given that rostral length and brightness of the lateral pelage are both correlated with age, the age bias could not be discarded as a putative cause of these differences between samples.

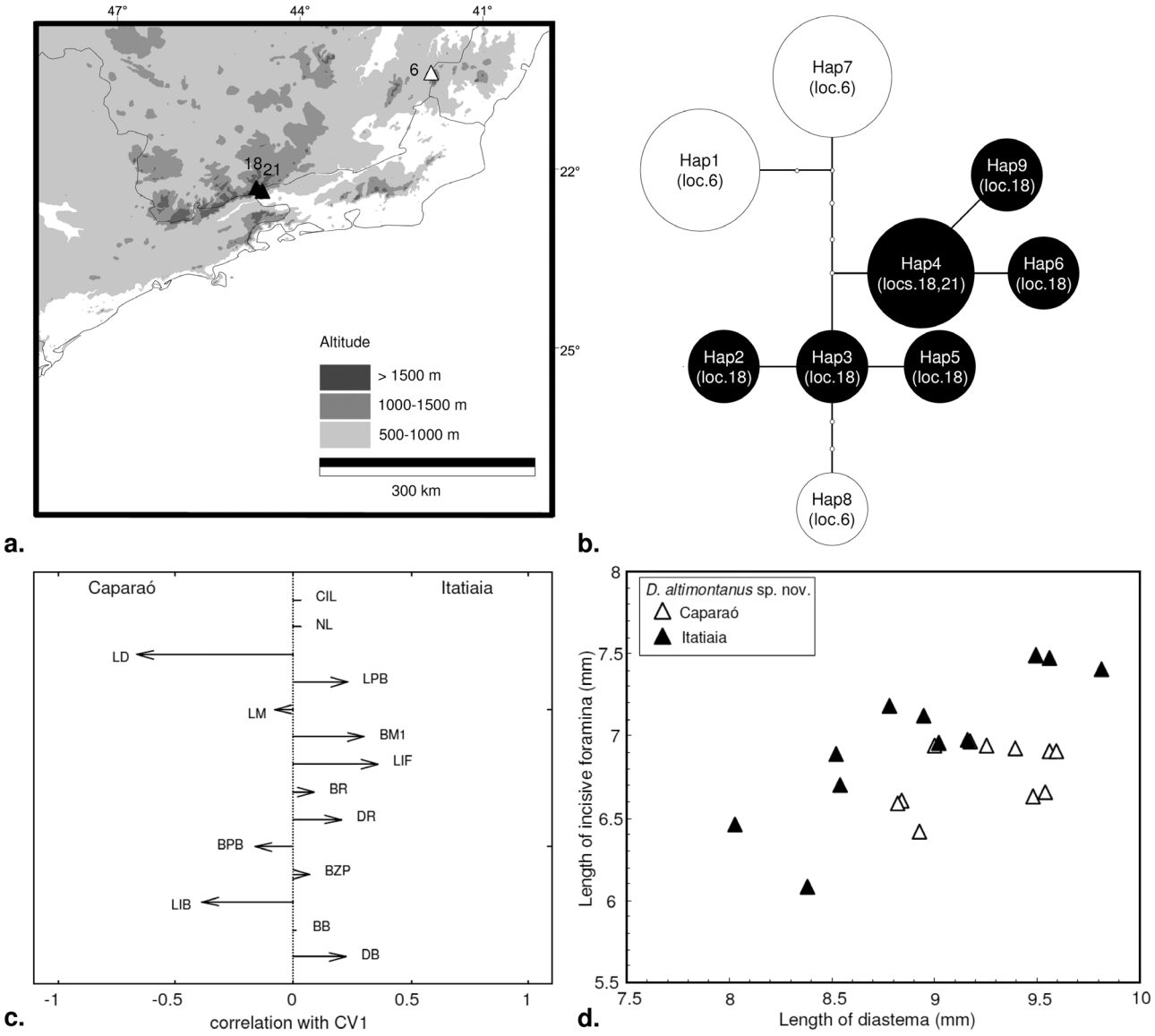

FIGURE 12. (a) Disjunct distribution of *D. altimontanus* and (b) statistical parsimony network depicting relationships between cytochrome *b* haplotypes from Caparaó (locality 6) and Itatiaia (localities 18, 21) mountain ranges. Circle sizes are proportional to haplotype frequencies and each line represents one mutational step. (c) Vector correlations among characters and CVA axes and (d) bivariate plot of most discriminant craniometric characters between Itatiaia and Caparaó populations.

Natural history. Little is known about life history aspects of *D. altimontanus*, most observations being based on habitat descriptions by collectors. At the Caparaó mountain range, Bonvicino *et al.* (1997) described the variation in small mammal species composition and abundance along the elevational gradient of 1000 to 2700 m. *Delomys altimontanus* (therein identified as *D. collinus*) was trapped at elevations higher than 1800 m, where it was frequently associated with humid montane forests and shrubs, and corresponded to 14.3 to 27.1% of the small mammals captured at these high altitude habitats. No captures were recorded at lower altitudinal zones (1400 to

1000 m), where submontane secondary forests predominated. Bonvicino *et al.* (1997) did not report any other species of *Delomys* at the Caparaó mountain range. Nevertheless, nearby records at lower elevations throughout Espírito Santo (localities 5 and 7) and Minas Gerais states (localities 9 and 10) suggest that *D. sublineatus* may occur sympatrically with *D. altimontanus* in the Caparaó region, but probably occupying the lower altitudinal zones and exhibiting limited syntopy with its mountaintop congener.

At the Itatiaia mountain range, *Delomys altimontanus* appears to be the only *Delomys* species recorded above 2100 m, on the altiplano dominated by *campos de altitude* vegetation (locality 21, Campos do Itatiaia) and scattered high-montane forests and shrubs. At these high elevations, however, we captured specimens of *D. altimontanus* solely in forested habitats near streams and never on the open *campos de altitude* formation. At lower elevations on Itatiaia (2000–1800 m), *D. altimontanus* is recorded in sympatry and syntopy with *D. dorsalis* (at localities 18 and 23, Brejo da Lapa and Abrigo Macieiras), where both species inhabit the humid montane forests characterized by the presence of the conifer *Araucaria angustifolia* and other cool-humid adapted austral plant taxa (Brade 1956). No specimens of *D. altimontanus* have been genetically or morphologically identified at elevations lower than 1800 m, so the altitudinal intervals occupied by this species in the two mountain ranges are apparently similar.

Remarks. The holotype of *D. dorsalis collinus* Thomas, 1917 (BMNH 14.2.22.12, skin and skull) was collected in 1913 by James Peter Hill at about 1470 m in the Itatiaia mountain range. Two other specimens of *Delomys* were also collected by Hill at Itatiaia: an adult female of *D. dorsalis* (BMNH 14.2.22.13, skin and skull) with 6 mammae and without altitude information, and an adult male of *D. altimontanus* (BMNH 14.2.22.11, skull only) with the specific locality of "Maceiro" (=Macieiras) written in the label. This last locality refers to an old resting place (former "Abrigo Macieiras"), located at approximately 1880 m altitude along the dirt road ("travessia Ruy Braga") that crossed the Itatiaia mountain range from the city of Itatiaia, in Rio de Janeiro state, to the city of Itamonte, in Minas Gerais state (Brade 1956). As this road was the main travelling route between the southern Rio de Janeiro and Minas Gerais states in this region during the beginning of the 20th century, it is probable that J. P. Hill obtained the three specimens of *Delomys* along its margins. The road originally traversed the Itatiaia range along the Maromba valley, where many rural properties and (later in 1937) the administrative base of the National Park of Itatiaia were established at lower elevations (900–1200 m).

Hershkovitz (1998) identified both *Delomys sublineatus* and *D. dorsalis collinus* amongst the specimens from Caparaó that Bonvicino *et al.* (1997) previously identified as "*D. collinus*". Nevertheless, the direct examination of this series and the inspection of the skulls and mandibles plates published in Hershkovitz (1998), confirms that all of Hershkovitz' specimens represent *D. altimontanus*.

Delomys dorsalis (Hensel 1872)

Hesperomys dorsalis Hensel (1872): 42
Hesperomys dorsalis obscura Leche (1886): 696
Akodon dorsalis: Trouessart (1898): 537 (new name combination)
Akodon dorsalis obscura: Trouessart (1898): 537 (new name combination)
Akodon dorsalis lechei Trouessart (1904): 434
Hesperomys (*Oryzomys*) *dorsalis*: Miranda-Ribeiro (1905): 187 (new name combination)
Thomasomys dorsalis: Thomas (1906): 443 (new name combination)
Delomys dorsalis: Thomas (1917): 196 (new name combination)
Delomys dorsalis collinus Thomas (1917): 197
Delomys dorsalis dorsalis: Gyldenstolpe (1932): 60 (new name combination)
Delomys dorsalis lechei: Gyldenstolpe (1932): 61 (new name combination)
Thomasomys dorsalis dorsalis: Ellerman (1941): 368 (new name combination)
Thomasomys dorsalis collinus: Ellerman (1941): 369 (new name combination)
Thomasomys dorsalis lechei: Ellerman (1941): 369 (new name combination)
Thomasomys lechei: Moojen (1952): 59
Thomasomys collinus: Moojen (1952): 60
Delomys collinus: Avila-Pires (1960): 32 (new name combination)

Emended diagnosis. A medium-sized species of the genus *Delomys* with soft and dense dorsal pelage, predominantly dark cinnamon-brown in color and without a bright yellow lateral line or patch; tail as long as head

and body; skull with pronounced rostrum and elongated nasal tube, formed by most of premaxillary length and projected beyond the gnathic process; supraorbital region exhibiting the fronto-parietal (coronal) suture discontinuous with the fronto-squamosal suture, forming an area of dorsal contact between the squamosal and the frontal; mandible with wide, deep, and asymmetrically excavated sigmoid notch, robust coronoid process and well-pronounced angular process; karyotype with 2n=82 and FN=80.

Distribution. The samples recognized here as *D. dorsalis* are distributed from the southernmost limits of the Brazilian Atlantic forest to the northernmost limits of the Serra do Mar, at the center of the Rio de Janeiro state. The distribution of *D. dorsalis* extends westward to the Misiones province in Argentina, but few records are available in the interior parts of Paraná and São Paulo states. Most collecting localities are situated along the coastal mountains covered by extensive humid montane and submontane forests, which in the Southern Highlands are frequently associated with the austral conifer *Araucaria angustifolia*. The submontane and montane forests in coastal Brazil occur at elevations of 30 to 1000 m between latitudes of 24°S and 32°S in the southernmost limit of the Brazilian Atlantic forest, but tend to occupy higher elevational intervals of 50 to 1500 m between the latitudes of 24°S and 14°S in Southeastern Brazil (Veloso *et al.* 1992). Likewise, the altitudinal distribution recorded for *D. dorsalis* in Southern Brazil varies from 57 m (locality 66) to 1700 m (locality 63), while in Southeastern Brazil, northern to the latitude of 24°S it varies from 650 (locality 44) to 1950 m (locality 27).

Variation in *Delomys dorsalis*. As previously evidenced by the molecular phylogenetic analyses, *D. dorsalis* exhibits an extensive molecular variation in relation to both *D. altimontanus* and *D. sublineatus*. Sixty-five haplotypes were identified among the 78 sequenced individuals of *D. dorsalis* sampled from 18 collecting localities, and their relationships suggest the recognition of three geographically defined intraspecific clades concordant with the distribution of the Mantiqueira, Serra do Mar and Southern mountain ranges in coastal Brazil (Fig. 13a). The quantitative results of the AMOVA analysis add further support to this spatial structure, indicating that a substantial component of the variation among haplotypes in *D. dorsalis* (80.9%; Φ_{CT}= 0.8091, p<0.001) is due to differentiation among the three regions rather than within these regions or within populations (7.64% and 11.45%, respectively; Φ_{SC}= 0.4002, p<0.001), with a significantly large fixation index among populations (Φ_{ST}= 0.8855, p<0.001).

The molecular diversity in the Mantiqueira and Serra do Mar clades is relatively reduced, as haplotypes within these regions average 0.45% and 0.64% pairwise genetic distance, respectively. The Southern clade, on the other hand, exhibits larger polymorphism, with haplotypes averaging 0.91% of pairwise genetic distance. The larger intraclade genetic distance in the Southern group is due to comparisons between haplotypes from the northernmost (states of São Paulo and Paraná) and southernmost localities (states of Santa Catarina and Rio Grande do Sul), which diverge by 1.47% pairwise genetic distance in average. However, the positive and significant correlations between genetic and geographic distances of populations assessed by a Mantel test (r = 0.91, p = 0.025) suggest that the artifactual sampling gap of collecting localities cannot be ruled out as the main cause of the genetic discontinuity between northernmost and southernmost populations in the Southern clade (de Queiroz & Good 1997).

Delomys dorsalis is also morphologically variable and, as previously mentioned, the number of mammary pairs does exhibit a discrete pattern of geographic variation within the species (Fig. 13b). The adult females examined from the Mantiqueira and Serra do Mar clades (n = 35) exhibit six mammae, while those from the Southern clade exhibit eight mammae (n = 19, including the Argentinean sample from Misiones), corroborating the pattern of variation described by Thomas (1917) and Voss (1993). The geographic transition between the two mammary conditions occurs around 23°50'S latitude, in the São Paulo state, and no population sampled in this region exhibits polymorphism of this trait (localities 36, 37 and 48). This transition is coincident with the latitudinal location of populations, but not fully congruent with the phylogenetic hierarchy within *D. dorsalis*, as the 6-mammae and 8-mammae lineages are not recovered as reciprocally monophyletic groups (Fig. 13c). A parsimony optimization (accelerated transformation) of mammary variation onto the molecular phylogeny of the genus, assuming the 8-mammae condition as primitive (Jansa & Weksler 2004; Weksler 2006), suggests two mammary number transformations along the evolutionary diversification of *Delomys*. The first would involve a loss of the pectoral pair in the ancestor of *D. altimontanus* and *D. dorsalis*, and the second would consist in a unique reacquisition of the pectoral pair (reversal) in the Southern clade of *D. dorsalis*. Nevertheless, since the close relationship between *D. altimontanus* and *D. dorsalis* has weak statistical support (<50% bootstrap values and 0.69 posterior probability), the mammary number transformations in *Delomys* are still uncertain and a better resolved phylogeny of the three species is needed for more conclusive character reconstructions.

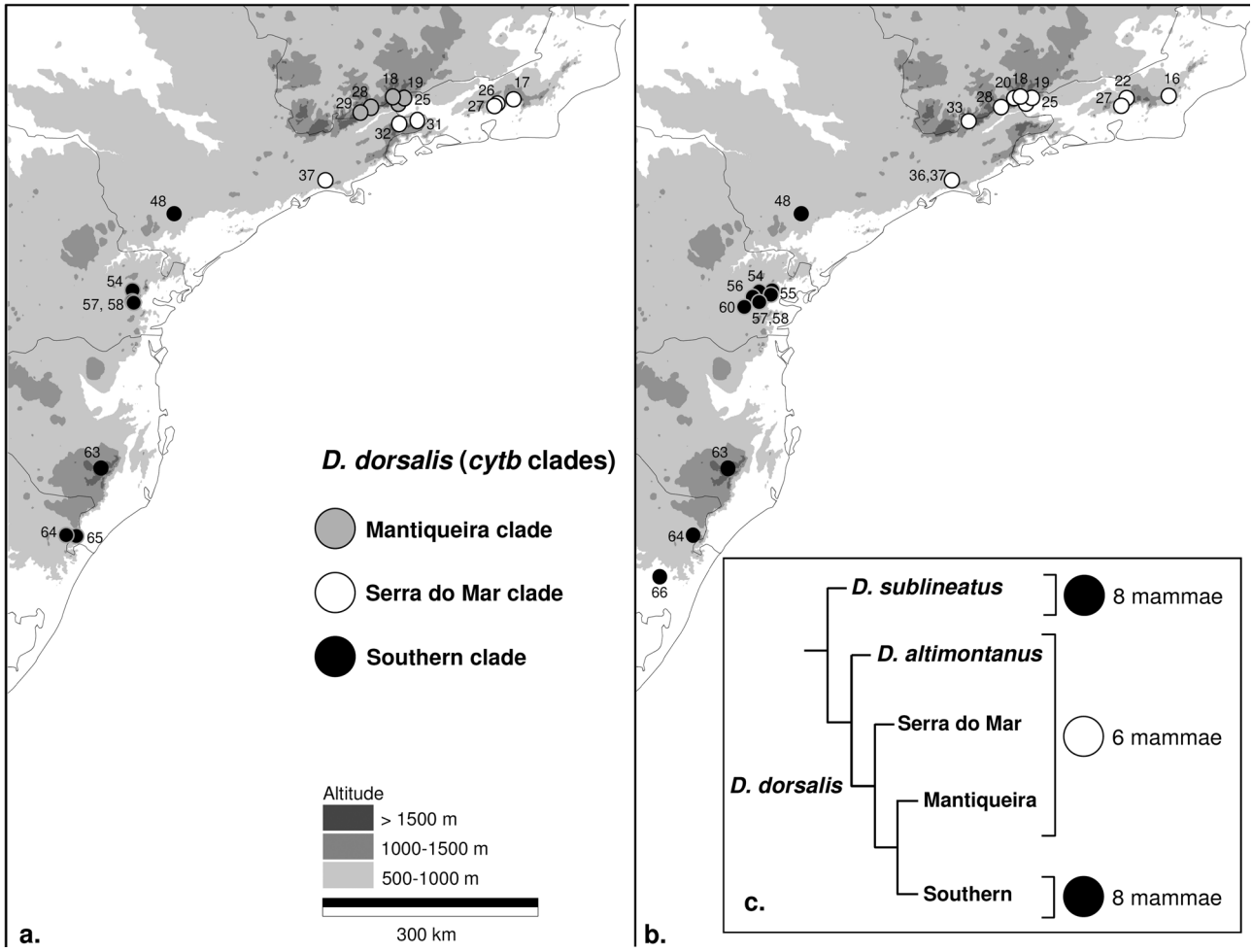

FIGURE 13. Distribution of (a) the intraspecific mitochondrial clades and (b) geographic variation in the number of mammae in *Delomys dorsalis* (white circles ─ 6 mammae; black circles ─ 8 mammae). The inset (c) shows the pectoral mammary pair variation mapped on the molecular phylogeny of *Delomys*.

A CVA including representatives of the Mantiqueira, Serra do Mar and Southern clades of *D. dorsalis*, including topotypes of *D. dorsalis* and the holotype of *D. d. collinus*, was carried out to test whether the craniometric variation among these three clades was congruent with their molecular or mammae number variation patterns. The three clades are depicted as three broadly overlapping clusters segregating along both CV1 and CV2, which account, respectively, for 70.2% and 29.8% of the among-group variation (Fig. 14a). The Mantiqueira clade diverges from Serra do Mar and Southern clades along CV2 by exhibiting longer molar toothrows (LM) and larger zygomatic plates (BZP) (Fig. 14b). Serra do Mar and Southern clades diverge along CV1 mostly due to variations in the interobital breadth (LIB), which is relatively wider in the Serra do Mar clade. Unlike the among-species CVA (Fig. 8) or the molecular phylogenies, however, craniometric discrimination among the *D. dorsalis* clades is less clear cut, with discriminant functions correctly allocating respectively 84.1%, 90.7% and 77.6% of the Mantiqueira, Serra do Mar and Southern clades representatives. Indeed, bivariate plots combining the most discriminant craniometric characters confirm a large overlap between Mantiqueira and Serra do Mar clades and between Mantiqueira and Southern clades (Figs. 14c–d). Therefore, craniometric variation among the three intraspecific lineages of *D. dorsalis* is too subtle to identify exclusive clusters in multivariate or bivariate analyses.

Despite the craniometric continuum among the three intraspecific clades, samples without genetic data could be allocated to one of the three geographic groups with moderate confidence levels. The *D. dorsalis* topotypes from Taquara (locality 66) were allocated to the Southern clade in 81% of the bootstrap iterations, while the holotype of *D. dorsalis collinus* and specimens from adjacent localities 20, 30 and 33 (Fig. 1) in Minas Gerais and São Paulo states were allocated to the Mantiqueira clade in all bootstrap iterations. Finally, a female of *D. dorsalis* with 8 mammae from a geographically distant locality in Argentina (locality 62) could also be confidently allocated to the Southern clade in all bootstrap iterations.

Thomas (1917) remarked on the length of upper molars as a distinctive trait for *D. d. collinus* (measured 5.0 mm by Thomas and 4.98 mm by us) in relation to Southern samples of *D. dorsalis* (measured 4.5–4.7 mm by Thomas). However, as shown in the bivariate plot (Fig. 14d), the Southern samples of *D. dorsalis* display a wider variation than that portrayed by Thomas (1917), weakening the value of dental measurements to diagnose *D. d. collinus.* In general, the craniometric variation among the three clades is subtle and no exclusive clusters representing the three *D. dorsalis* clades could be identified in the multivariate and bivariate combinations of characters (Fig. 14).

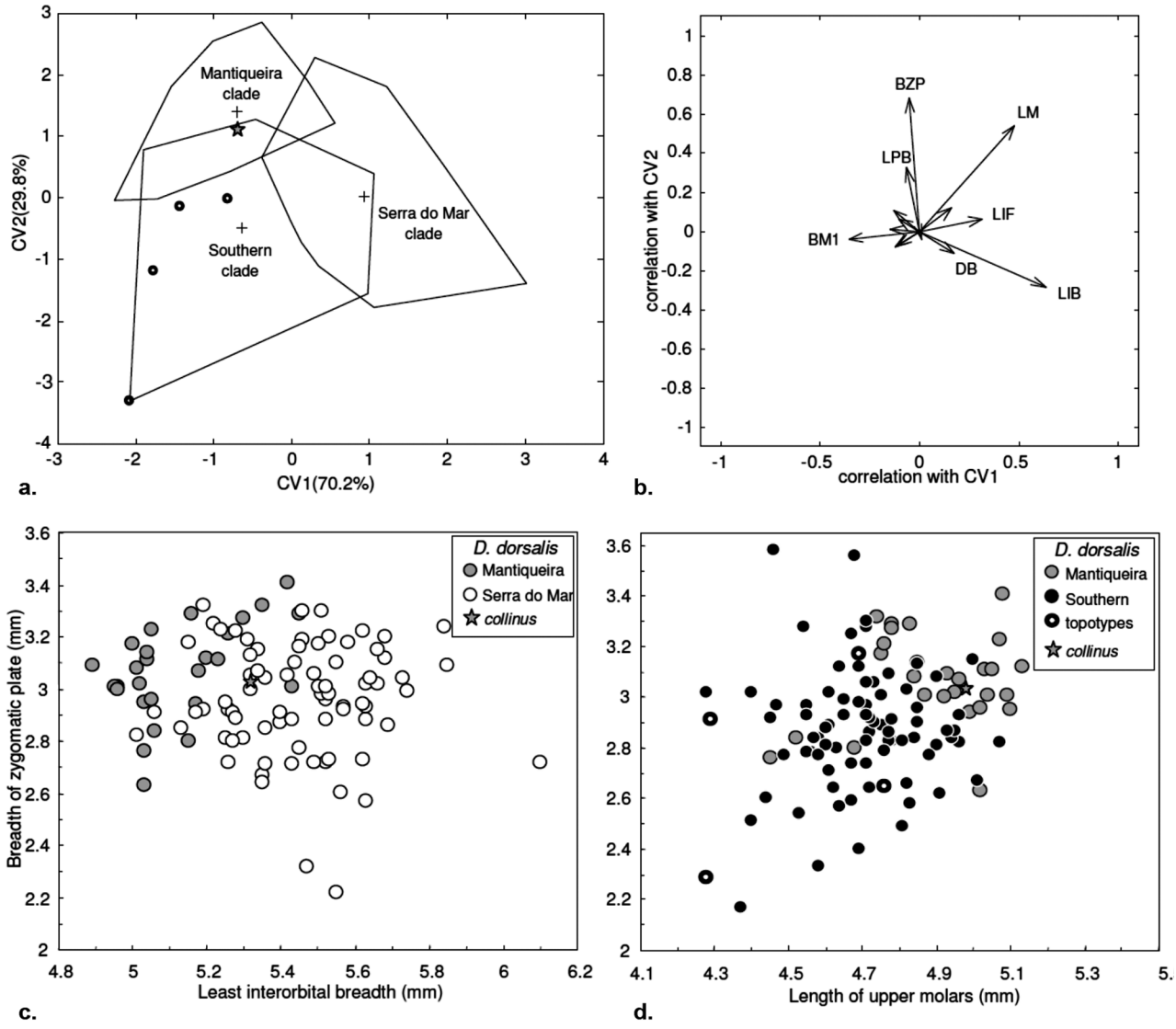

FIGURE 14. Craniometric discrimination among intraspecific clades of *D. dorsalis:* (a) CVA analysis among the three clades and (b) respective vector correlations among characters and CVA axes. Bivariate plot of the two most discriminant craniometric characters (c) between the Mantiqueira and Serra do Mar clades, and (d) between the Mantiqueira and Southern clades, also depicting the allocation of taxonomically important samples.

In the light of the current molecular and morphological evidence, applying the name *D. dorsalis collinus* to the 6-mammate specimens from Mantiqueira and Serra do Mar, as originally envisioned by Thomas (1917) and Voss (1993), would render this subspecies paraphyletic or dyphyletic respective to 8-mammate *D. dorsalis dorsalis*. An alternative would be to restrict *D. dorsalis collinus* to the Mantiqueira clade and *D. dorsalis dorsalis* to the Southern clade, describing the Serra do Mar clade as a distinct subspecies. Although more congruent with the number of lineages in *D. dorsalis*, this last option does not seem practical, since the recognition of subspecies would be fully dependent on molecular data in the absence of diagnostic morphological characters between the Serra do Mar and Mantiqueira populations. Voss (1993) reported a high frequency of specimens from Boracéia and

Casa Grande, in São Paulo state, with white tipped tails. This condition was not found in other samples from Serra do Mar examined by us, such as those from Teresópolis or Parati, in the Rio de Janeiro state, and may rather be a locally polymorphic character. The Serra do Mar clade is also polymorphic for tail color pattern, with a higher frequency (57%) of weakly bicolored tails in samples from Alto da Serra, Boracéia and Casa Grande, while other samples of this clade exhibit higher frequencies (>60%) of strongly bicolored tails. Given the current uncertainty in the morphological discrimination among the three clades of *D. dorsalis*, we opted not to formally recognize subspecies based on them, and regard *D. dorsalis collinus* as a junior synonym of *D. dorsalis*.

Discussion

The genetic and morphological patterns described here are largely congruent with the recognition of three species in the genus *Delomys*, each of which is karyotypically and morphologically diagnosable, even in localities of sympatry or syntopy, such as in the high-altitude zones of Itatiaia (~1800m). The analysis of biological diversity under an integrative approach, combining morphological and molecular data, as applied here to the genus *Delomys*, also revealed fine-scale biogeographic patterns in the Atlantic forest which suggest a causal role of montane habitats in fostering biological diversity in this region. Tropical mountain systems are known to have served as allopatric refuges for cold-adapted taxa during periods of warmer climates, such as the Quaternary interglacials, setting the stage for allopatric divergence and speciation between populations isolated on different mountaintops (Roy 1997; Gonçalves *et al.* 2007; Smith & Patton 2007; Safford 1999, 2007). During glacial periods, montane populations would have expanded their distributions to the lowlands (Behling 2002; Ledru *et al.* 2005), and if reproductive incompatibility had not evolved during the isolation, they could restitute gene flow and gradually homogenize differences accumulated in the last interglacial. The population geographic structure and disjunct distributions of *D. altimontanus* and *D. dorsalis* are interesting in this regard because they exemplify two stages of the allopatric differentiation process.

Delomys altimontanus is restricted to the two highest mountaintops in Southerastern Brazil, which are 300 km apart from each other, but the genetic evidence indicates that isolated populations are not reciprocally monophyletic or geographically structured, also exhibiting low levels of pairwise genetic divergence. Therefore, the populations of *D. altimontanus* might have experienced recent gene flow, possibly during the last glacial period when the species was more broadly distributed across Southeastern Brazil. Since then, their posterior isolation to mountaintops during the Holocene is apparently too recent to have produced patterns of reciprocal monophyly and complete sorting of mitochondrial lineages between populations.

Delomys dorsalis, on the other hand, is spatially structured in three geographic groups that are concordant with the Mantiqueira, Serra do Mar and Southern mountain ranges. The three molecular clades in this case might have resulted from past disjunctions among humid montane forests that extended long enough to produce monophyletic geographical groups of mitochondrial lineages. Assuming that the cytochrome *b* gene has evolved at about the same rate in all *Delomys* species, the disjunctions among *D. dorsalis* populations are apparently more ancient than that between the Caparaó and Itatiaia populations of *D. altimontanus*, and their divergence might have been maintained even during glacial periods when montane taxa would have been more widely distributed. The more pronounced divergence among *D. dorsalis* populations is also evident in the variation of mammae number between northern (Serra do Mar and Mantiqueira) and southern populations. Litter-size and parental investment may be implicated in mammae number in rodents (Gilbert 1986), and the variation among *D. dorsalis* populations could thus reflect distinct life-histories. Reproductive studies of populations of *D. dorsalis* from the Southern clade shows that 8-mammae females exhibited 2 to 5 embryos (Cademartori *et al.* 2005), while 6-mammae pregnant females collected in the Serra do Mar (locality 37, information recorded in the specimen-label by the collectors) recorded 1 to 3 embryos. If this information is corroborated by additional populations from Mantiqueira and Serra do Mar, the 8-mammae condition in the Southern populations could be an adaptation to food supply or other ecological factors prompting larger clutch-sizes.

The patterns recovered here also call attention to the restricted geographic ranges of *D. altimontanus* and other altitudinally restricted mammal species in the Atlantic forest (e.g. *Juliomys rimofrons*, *Akodon mystax*, *Oxymycterus caparaoe*; Oliveira & Bonvicino 2002; Gonçalves *et al.* 2007), which may be highly vulnerable to local disturbances on montane habitats, such as fires and grazing, and hence eligible to IUCN endangerment categories.

Acknowledgements

We are grateful to Bruce Patterson (FMNH), James Patton (MVZ), Gisele Lessa (MZUFV), Helio Fernandes (MBML), Mario de Vivo (MZUSP), Paula Jenkins (BMNH), Valéria Tavares (UFMG) and Tereza Cristina Castellano Margarido (MHNCI) for allowing access to the mammal collections. We are indebited to Lena Geise, Cibele Bonvicino, Yuri Leite, James Patton and Renata Pardini for providing tissue samples from recently collected specimens. We also thank Adriana Bueno, Cibele Bonvicino, Edmar Manduca, Julio Vilela, Jânio Moreira, Laura Naxara, Liliani Tiepolo, Maria Olímpia G. Lopes and Renata Pardini for their help during field work, and Carina Azevedo for her assistance with the karyograms. Marcelo Weksler, Robert Voss and an anonymous reviewer gave important suggestions on a previous version of this manuscript. Collecting licenses in Caparaó and Itatiaia national parks (070/2003 and 143/2004) were provided by Instituto Brasileiro de Meio Ambiente e de Recursos Naturais Renováveis. Funding was provided by Conselho Nacional de Pesquisa e Desenvolvimento Tecnológico (CNPq, processes 45379/2010-7 and 481869/2008-5) and Fundação Carlos Chagas Filho de Amparo à Pesquisa do Rio de Janeiro (FAPERJ Processes E-26/110.605/2009 and E-26/111.404/2012). PRG benefited from a doctoral and a postdoctoral fellowship from CNPq (processes 201.268/2004-3 and 160.050/2007-3), and JAO benefited from research fellowships from CNPq (processes 3068801/2007 and 306935/2010-4).

References

Ashkenazy, H., Penn, O., Doron-Faigenboim, A., Cohen, O., Cannarozzi G., Zomer, O. & Pupko, T. (2012) FastML: a web server for probabilistic reconstruction of ancestral sequences. *Nucleic Acids Research*, 40, W580–584. http://dx.doi.org/10.1093/nar/gks498

Avila-Pires, F.D. (1960) Roedores colecionados na região de Lagoa Santa, Minas Gerais, Brasil. *Arquivos do Museu Nacional*, 50, 25–45.

Avise, J.C. (2000) *Phylogeography: the history and formation of species*. Harvard University Press, Massachusetts, 447 pp.

Baker, R.J. & Bradley, R.D. (2006) Speciation in mammals and the genetic species concept. *Journal of Mammalogy*, 87, 643–662.

Behling, H. (2002) South and southeast Brazilian grasslands during Late Quaternary times: a synthesis. *Palaeogeography, Palaeoclimatology, Palaeoecology*, 177, 19–27. http://dx.doi.org/10.1016/s0031-0182(01)00349-2

Bonvicino, C.R. & Geise, L. (1995) Taxonomic status of *Delomys dorsalis collinus* Thomas, 1917 (Rodentia, Cricetidae) and description of a new karyotype. *Zeitschrift für Säugetierkunde*, 60, 124–127.

Bonvicino, C.R., Langguth, A., Lindbergh, S.M. & Paula, A.C. (1997) An elevational gradient study of small mammals at Caparaó National Park, South eastern Brazil. *Mammalia*, 61, 547–560.

Bonvicino, C.R., D'Andrea, P.S. & Borodin, P.M. (2001) Pericentric inversion in natural populations of *Oligoryzomys nigripes* (Rodentia: Sigmodontinae). *Genome*, 44, 791–796. http://dx.doi.org/10.1139/gen-44-5-791

Bonvicino, C.R., Gonçalves, P.R., Oliveira, J.A., Oliveira, L.F.B. & Mattevi, M.S. (2009) Divergence in *Zygodontomys* (Rodentia: Sigmodontinae) and distribution of Amazonian Savannas. *Journal of Heredity*, 100, 322–328. http://dx.doi.org/10.1093/jhered/esn105

Brade, A.C. (1956) A flora do Parque Nacional do Itatiaia. *Boletim do Parque Nacional do Itatiaia*, 5, 1–112.

Cademartori, C.V., Fabián, M.E. & Manegheti, J.O. (2005) Biologia reprodutiva de *Delomys dorsalis* (Hensel, 1872) - Rodentia, Sigmodontinae - em área de floresta ombrófila mista, Rio Grande do Sul, Brasil. *Mastozoología Neotropical*, 12, 133–144.

Clement, M., Posada, D. & Crandall, K.A. (2000) TCS: a computer program to estimate gene genealogies. *Molecular Ecology*, 9, 1657–1659. http://dx.doi.org/10.1046/j.1365-294x.2000.01020.x

Costello, M.J., May, R.M. & Stork, N.E. (2013) Can we name Earth's species before they go extinct? *Science*, 339, 413–416.

Darriba, D., Taboada, G.L., Doallo, R. & Posada, D. (2012) jModelTest 2: more models, new heuristics and parallel computing. *Nature Methods*, 9, 772. http://dx.doi.org/10.1038/nmeth.2109

De Blase, A.F. & Martin, R.E. (1981) *A Manual of Mammalogy, with keys to families of the world*, *Second Edition*. Wm. C. Brown Company Publishers, Dubuque, Iowa, 445 pp.

D'Elía, G., Pardiñas, U.F.J., Teta, P. & Patton, J.L. (2007) Definition and diagnosis of a new tribe of sigmodontine rodents (Cricetidae: Sigmodontinae), and a revised classification of the subfamily. *Gayana*, 71, 187–194. http://dx.doi.org/10.4067/s0717-65382007000200007

de Queiroz, K. & Good, D.A. (1997) Phenetic clustering in biology: a critique. *The Quarterly Review of Biology*, 72, 1–30.

Delciellos, A.C., Novaes, R.L.M., Loguercio, M.F.C., Geise, L., Santori, R.F., Souza, R.F., Papi, B.S., Raíces, D., Vieira, N.R., Felix, S., Detogne, N., Silva, C.C.S., Bergallo, H.G. & Rocha-Barbosa, O. (2012) Mammals of Serra da Bocaina National Park, state of Rio de Janeiro, southeastern Brazil. *Checklist*, 8, 675–692.

Ellerman, J.R. (1941) *The families and genera of living rodents with a list of named forms by R. W. Hayman and G. W. C. Holt (1758–1936)*. *Vol. 2. Family Muridae.* British Museum (Natural History), London, 690 pp.

Excoffier, L., Laval, L.G. & Schneider, S. (2005) Arlequin ver. 3: An integrated software package for population genetics data analysis. *Evolutionary Bioinformatics Online*, 1, 47–50.

Felsenstein, J. (1985) Confidence limits on phylogenies: an approach using the bootstrap. *Evolution*, 39, 783–791. http://dx.doi.org/10.2307/2408678

Ford, C.E. & Hamerton, J.L. (1956) A colchicine hypotonic citrate squash sequence for mammalian chromosomes. *Stain Technology*, 31, 247–251. http://dx.doi.org/10.3109/10520295609113814

Geise, L., Pereira, L.G., Bossi, D.E.P. & Bergallo, H.G. (2004) Pattern of elevational distribution and richness of nonvolant mammals in Itatiaia National Park and surroundings, in southeastern Brazil. *Brazilian Journal of Biology*, 64, 92–101.

Gilbert, A.N. (1986) Mammary number and litter size in Rodentia: the one-half rule. *Proceedings of the National Academy of Sciences, USA*, 83, 4828–4830.

Gonçalves, P.R., Myers, P., Vilela, J.F. & Oliveira, J.A. (2007) Systematics of species of the genus *Akodon* (Rodentia: Sigmodontinae) in Southeastern Brazil and implications for the biogeography of the campos de altitude. *Miscellaneous Publications Museum of Zoology, University of Michigan*, 197, 1–24.

Gyldenstolpe, N. (1932) A manual of neotropical sigmodont rodents. *Kungliga Svenska Ventenskapsakad Handlingar*, 3, 1–164.

Hensel, R. (1872) *Beiträge zur Kenntniss der Säugethiere Süd-Brasiliens*. Königlichen Akadademie der Wissenschaften, Berlin, 130 pp.

Hershkovitz, P. (1998) Report on some sigmodontine rodents collected in southeastern Brazil with descriptions of a new genus and six new species. *Bonner Zoologische Beiträge*, 47, 193–256.

Jansa, S.A. & Weksler, M. (2004) Phylogeny of muroid rodents: relationships within and among major lineages as determined by IRBP gene sequences. *Molecular Phylogenetics and Evolution*, 31, 256–276. http://dx.doi.org/10.1016/j.ympev.2003.07.002

Leche, W. (1886) Ueber einige südbrasilianische *Hesperomys*-Arten. *Zoologische Jahrbücher*, 1, 687–702.

Ledru, M.P., Rousseau, D.D., Cruz, J., Riccomini, C., Karmann, I. & Martin, L. (2005) Paleoclimate changes during the last 100,000 yr from a record in the Brazilian Atlantic rainforest region and interhemispheric comparison. *Quaternary Research*, 64, 444–450. http://dx.doi.org/10.1016/j.yqres.2005.08.006

Levan, A., Fredga, K. & Sandberg, A.A. (1964) Nomenclature for centromeric position on chromosomes. *Hereditas*, 52, 201–220. http://dx.doi.org/10.1111/j.1601-5223.1964.tb01953.x

Manly, B.F.J. (1994) *Multivariate statistical methods a primer*. Chapman & Hall, London, 215 pp.

Miranda-Ribeiro, A. (1905) Vertebrados do Itatiaya (Peixes, Serpentes, Saurios, Aves e Mammiferos). *Archivos do Museu Nacional*, 13, 165–190.

Modesto, T.C., Pessoa, F.S., Enrici, M.C., Attias, N., Costa, L.D.M., Albuquerque, H.G. & Bergallo, H.G. (2008) Mamíferos do Parque Estadual do Desengano, Rio de Janeiro, Brasil. *Biota Neotropica*, 8, 153–159.

Moojen, J. (1952) *Os Roedores do Brasil*. Instituto Nacional do Livro, Rio de Janeiro, 214 pp.

Moreira, J.C., Manduca, E.G., Gonçalves, P.R., Morais, M.M.J., Pereira, R.F., Lessa, G. & Dergam, J.A. (2009) Small mammals from Serra do Brigadeiro state park. *Arquivos do Museu Nacional*, 67, 103–118.

Musser, G.G. & Carleton, M.D. (2005) Family Cricetidae. *In*: Wilson, D.E. & Reeder, D.H. (Eds.), *Mammal Species of the World*: *a taxonomic and geographic reference*, *Third Edition*. Smithsonian Institution Press, Washington, pp. 894–1531.

Myers, P., Patton, J.L. & Smith, M.F. (1990) A review of the *boliviensis* group of *Akodon* (Muridae: Sigmodontinae), with emphasis on Peru and Bolivia. *Miscellaneous Publications Museum of Zoology, University of Michigan*, 177, 1–104.

Olifiers, N., Eduardo, C., Grelle, V., Bonvicino, C.R., Geise, L., Pereira, L.G. & Cerqueira, R. (2007) Pequenos mamíferos não-voadores do Parque Nacional da Serra dos Órgãos. *In*: Cronemberger, C. & Viveiros de Castro, E.B. (Eds.), *Ciência e Conservação na Serra dos Órgãos*. IBAMA, Brasilia, pp. 188–192.

Oliveira, J.A. & Bonvicino, C.R. (2002) A new species of sigmodontine rodent from the Atlantic forest of eastern Brazil. *Acta Theriologica*, 47, 307–322. http://dx.doi.org/10.1007/bf03194149

Paglia, A.P., Fonseca, G.A.B., Rylands, A.B., Herrmann, G., Aguiar, L.M.S., Chiarello, A.G., Leite, Y.L.R., Costa, L.P., Siciliano, S., Kierulff, M.C., Mendes, S.L., Tavares, V.C., Mittermeier, R.A. & Patton, J.L. (2012) *Annotated checklist of Brazilian Mammals*. 2nd Edition, *Occasional Papers in Conservation Biology No. 6*, Conservation International, Arlington, VA, 76 pp.

Parada, A, Pardiñas, U.F.J., Salazar-Bravo, J., D'Elía, G. & Palma, R.E. (2013) Dating an impressive Neotropical radiation: molecular time estimates for the Sigmodontinae (Rodentia) provide insights into its historical biogeography. *Molecular Phylogenetics and Evolution*, 66, 960–968. http://dx.doi.org/10.1016/j.ympev.2012.12.001

Pardiñas, U.F.J. (2008) A new genus of oryzomyine rodent (Cricetidae: Sigmodontinae) from the Pleistocene of Argentina. *Journal of Mammalogy*, 89, 1270–1278.
http://dx.doi.org/10.1644/07-mamm-a-099.1

Percequillo, A.R., Weksler, M. & Costa, L.P. (2011) A new genus and species of rodent from the Brazilian Atlantic Forest (Rodentia: Cricetidae: Sigmodontinae: Oryzomyini), with comments on oryzomyine biogeography. *Zoological Journal of the Linnean Society*, 161, 357–390.
http://dx.doi.org/10.1111/j.1096-3642.2010.00643.x

Pine, R.H., Timm, R.M. & Weksler, M. (2012) A newly recognized clade of trans-Andean Oryzomyini (Rodentia: Cricetidae), with description of a new genus. *Journal of Mammalogy*, 93, 851–870.
http://dx.doi.org/10.1644/11-mamm-a-012.1

Reeder, D.A., Helgen, K.M. & Wilson, D.E. (2007) Global trends and biases in new mammal species discoveries. *Occasional Papers*, *Museum of Texas Tech University*, 269, 1–40.

Ronquist, F., Teslenko, M., van der Mark, P., Ayres, D.L., Darling, A., Hahna, S., Larget, B., Liu, L., Suchard, M.A. & Huelsenbeck, J.P. (2012) MrBayes 3.2: efficient Bayesian phylogenetic inference and model choice across a large model space. *Systematic Biology*, 61, 539–542.

Roy, M.S. (1997) Recent diversification in African greenbuls (Pycnonotidae: *Andropadus*) supports a montane speciation model. *Proceedings of the Royal Society, London, Series B* 264, 1337–1344.
http://dx.doi.org/10.1098/rspb.1997.0185

Safford, H.D. (1999) Brazilian Paramos I. An introduction to the physical environment and vegetation of the campos de altitude. *Journal of Biogeography*, 26, 693–712.
http://dx.doi.org/10.1046/j.1365-2699.1999.00313.x

Safford, H.D. (2007) Brazilian Páramos IV. Phytogeography of the campos de altitude. *Journal of Biogeography* 34, 1701–1722.

Sambrook, J., Fritsch, E.F. & Maniatis, T. (1989) *Molecular cloning: a laboratory manual*. Cold Spring Harbor Laboratory Press, Cold Spring Harbor, New York, 1626 pp.

Smith, M.F. & Patton, J.L. (1993) The diversification of South American murid rodents: evidence from mitocondrial DNA sequence data for the akodontine tribe. *Biological Journal of the Linnean Society*, 50, 149–177.
http://dx.doi.org/10.1111/j.1095-8312.1993.tb00924.x

Smith, M.F. & Patton, J.L. (2007) Molecular phylogenetics and diversification of South American grass mice, genus *Akodon*. *In*: Kelt, D.A., Lessa, E.P., Salazar-Bravo, J. & Patton, J.L. (Eds.), *The Quintessential Naturalist: Honoring the Life and Legacy of Oliver P. Pearson*. University of California Press, Berkeley, pp. 827–858.

Strauss R.E. (1999) Matlab statistical functions. Available from: http://www.faculty.biol.ttu.edu/ Strauss/Matlab/matlab.htm (accessed 2 May 2012)

Tamura, K., Dudley, J., Nei, M. & Kumar, S. (2007) MEGA4: Molecular Evolutionary Genetics Analysis (MEGA) Software Version 4.0. *Molecular Biology and Evolution*, 24, 1596–1599.
http://dx.doi.org/10.1093/molbev/msm092

Thomas, O. (1903) Notes on Neotropical mammals of the genera *Felis, Hapale, Oryzomys, Akodon* and *Ctenomys*, with descriptions of new species. *Annals and Magazine of Natural History*, 7 (12), 234–243.
http://dx.doi.org/10.1080/00222930308678847

Thomas, O. (1906) Notes on South American rodents. III. A new *Oecomys* and two new species of *Holochilus*. *Annals and Magazine of Natural History*, 7 (18), 442–448.

Thomas, O. (1917) On the arrangement of South American rats allied to *Oryzomys* and *Rhipidomys*. *Annals and Magazine of Natural History*, 8 (20), 192–198.

Trouessart, E.-L. (1898) *Catalogus mammalium tam viventium quam fossilium*. R. Friedländer & Sohn, Berlin, 664 pp.

Trouessart, E.-L. (1904) *Catalogus mammalium tam viventium quam fossilium, quinquennale supplementum*. R. Friedländer & Sohn, Berlin, 929 pp.

Veloso, H.P., Filho, L.C.O., Vaz, A.M.S.F., Lima, M.P.M., Marquete, R. & Brazão, J.E.M. (1992) *Manual técnico da vegetação brasileira*. Fundação Instituto Brasileiro de Geografia e Estatística, Rio de Janeiro, 92 pp.

Voss, R.S. (1988) Systematics and ecology of ichthyomyine rodents (Muroidea), patterns of morphological evolution in a small adaptive radiation. *Bulletin of the American Museum of Natural History*, 188, 259–493.

Voss, R.S. (1991) An introduction to the Neotropical muroid rodent genus *Zygodontomys*. *Bulletin of the American Museum of Natural History*, 210, 1–113.

Voss, R.S. (1993) A revision of the Brazilian Muroid Rodent genus *Delomys* with remarks on "Thomasomyine" characters. *American Museum Novitates*, 3073, 1–44.

Weksler, M. (2006) Phylogenetic relationships of Oryzomine rodents (Muroidea: Sigmodontinae): separate and combined analyses of morphological and molecular data. *Bulletin of the American Museum of Natural History*, 296, 1–149.
http://dx.doi.org/10.1206/0003-0090(2006)296[0001:proorm]2.0.co;2

Weksler, M. Percequillo, A.R. & Voss, R.S. (2006) Ten new genera of Oryzomyine rodents (Cricetidae, Sigmodontinae). *American Museum Novitates,* 3537, 1–29.
http://dx.doi.org/10.1206/0003-0082(2006)3537[1:tngoor]2.0.co;2

Zanchin, N.I.T., Sbalqueiro, I.J., Langguth, A., Bossle, R.C., Castro, E.C., Oliveira, L.F.B. & Mattevi, M.S. (1992) Karyotype and species diversity of the genus *Delomys* (Rodentia, Cricetidae) in Brazil. *Acta Theriologica*, 37, 163–169.

Zwickl, D.J. (2006) *Genetic algorithm approaches for the phylogenetic analysis of large biological sequence datasets under the maximum likelihood criterion*. The University of Texas at Austin, Austin, 115 pp.

APPENDIX

Gazetteer of collecting localities and specimens examined. Numbers in brackets refers to localities mapped in Fig. 1. Localities are numbered from north to south, followed by latitude and longitude (south and west, respectively, in negative decimal degrees), elevation in meters and samples sizes of morphologically (*morph*) and molecularly (*mtDNA*) analyzed specimens. Uncatalogued specimens will be deposited in the collections of the Museu Nacional, Universidade Federal do Rio de Janeiro (HGB, LG, JAO, M), and the Museu de Zoologia, Universidade de São Paulo (AB, EBB).

Delomys altimontanus

[6**]** Parque Nacional do Caparaó (includes Terreirão-Segredo-Arrozal-Cachoeira Bonita), Alto Caparaó, MG (Caparaó Mt.), (-20.4339ºS, -41.8494ºW, 2500m), (*morph* = 13), (*mtDNA* = 8): FMNH uncatalogued (PH10024, 10029, 10066, 10080, 10089, 10180, 10190, 10219, 10373, 10433, 10434, 10437), MN69592.

[18**]** Brejo da Lapa (includes Hotel Alsene), Itamonte, MG (Itatiaia Mt.), (-22.3483ºS, -44.6939ºW, 1843m), (*morph* = 14), (*mtDNA* = 5): MN uncatalogued (LG106, 205), MN33698−33702, 60573−60576, 60584, 60585, 79013.

[21**]** Campos do Itatiaia (Abrigo Rebouças), Parque Nacional do Itatiaia, RJ (Itatiaia Mt.), (-22.3906ºS, -44.6706ºW, 2450m), (*morph* = 3), (*mtDNA* = 2): MN69712, 69746, MZUSP2163.

[23**]** Abrigo Macieiras, Parque Nacional do Itatiaia, RJ (Itatiaia Mt.), (-22.4165ºS, -44.6442ºW,1880m), (*morph* = 1): BMNH14.2.23.11.

Delomys dorsalis

[16**]** Serra de Macaé, Macaé, RJ, (-22.3167ºS, -42.3333ºW, 1200m), (*morph* = 3): MZUSP2786−2787, 2789.

[17**]** Parque Estadual dos Três Picos, Salinas/Nova Friburgo, RJ, (-22.3473ºS, -42.7383ºW,1600m), (*morph* = 7), (*mtDNA* = 7): MN80378, 80393, 80396, 80397, 80410, 80411, 80415.

[18**]** Brejo da Lapa, Itamonte, MG (Itatiaia Mt.), (-22.3483ºS, -44.6939ºW, 1843m), (*morph* = 20), (*mtDNA* = 13): MN44058, 44059, 44062−44064, 60572, 60577−60583, 60586, 60588, 60589, 70048, 70049, 79005, 79021.

[19**]** Serrinha do Anambari, Itatiaia, RJ (Itatiaia Mt.), (-22.3667ºS, -44.5500ºW, 850m), (*morph* = 1), (*mtDNA* = 1): MN (HGB 64).

[20**]** Posses, 13km SE Itanhandú, MG, (-22.3813ºS, -44.8380ºW, 1600m), (*morph* = 1): UFMG1876.

[22**]** Faz. C. Guinle, Teresópolis, RJ, (-22.4122ºS, -42.9656ºW, 900m), (*morph* = 23): FMNH53871, 53872, MN11608, 11609, 11665, 6339, 7001, 7004, 7005, 7007−7013, 7015, 7016, 7064, 7082, 7085, 7087, 7089.

[23**]** Abrigo Macieiras, Parque Nacional do Itatiaia, RJ (Itatiaia Mt.), (-22.4165ºS, -44.6442ºW, 1880m), (*morph* = 1): BMNH14.2.23.13.

[24**]** Subaio, Teresópolis, RJ, (-22.4358ºS, -42.9317ºW, 1050m), (*morph* = 1): MN uncatalogued (JAO230).

[25**]** Maromba, Itatiaia, RJ (Itatiaia Mt.), (-22.4384ºS, -44.6245ºW, 1170m), (*morph* = 6), (*mtDNA* = 4): BMNH14.2.23.12, MN uncatalogued (HGB-DB 19, 20), MN78909, 78915, 78927.

[26**]** Parque Nacional da Serra dos Órgãos (Paquequer), Teresópolis, RJ, (-22.4547ºS, -42.9972ºW, 1000m), (*morph* = 14), (*mtDNA* = 3): MN70005, 70006, 70008, 70009, 700012, 700013, 70016, 70019, 70028, 70029−70031, 70033, 70034.

[27**]** Parque Nacional da Serra dos Órgãos (Vale das Antas), Teresópolis, RJ, (-22.4639ºS, -43.0425ºW, 1950m), (*morph* = 11), (*mtDNA* = 3): MN70127, 70128, 70130−70133, 70139, 70149-70152.

[28**]** Fazenda do Itaguaré, 10-16km SW Passa Quatro, MG, (-22.4667ºS, -45.0833ºW, 1500m), (*morph* = 5), (*mtDNA* = 2): UFMG1868−1870, 1872, 1873.

[29**]** Fazenda da Onça, 13km SW Delfim Moreira, MG, (-22.5531ºS, -45.2673ºW, 1850m), (*morph* = 2), (*mtDNA* = 2): UFMG1874, 1875.

[30**]** Piquete, SP, (-22.6000ºS, -45.1833ºW, 800m), (*morph* = 1): BMNH1.6.6.43.

[31**]** Estação Ecológica do Bananal, Bananal, SP, (-22.6836ºS, -44.3233ºW, 800m), (*morph* = 2), (*mtDNA* = 2): MZUSP uncatalogued (EEB711, 712).

[32**]** Parque Nacional da Bocaina, São José do Barreiro, SP, (-22.7200ºS, -44.6150ºW, 1400m), (*morph* = 1), (*mtDNA* = 1): MN (HGB DB 18).

[33**]** Campos do Jordão, SP, (-22.7394ºS, -45.5914ºW, 1600m), (*morph* = 9): MZUSP2103, 2105−2111, 2114.

[34**]** Pedra Branca, Parati, RJ, (-23.2178ºS, -44.7131ºW,800m), (*morph* = 15): MN6207, 6211, 6213, 6224, 6226, 6290, 8147−8149, 8408, 8409, 8414, 8416, 8419, 8420.

[36**]** Casa Grande, Biritiba Mirim, SP, (-23.5725ºS, -46.0386ºW,850m), (*morph* = 19): FMNH136940, MN32450, MZUSP22796, 22810, 22811, UFMG0006, 0009, 0012, 0017, 0018, 0037, 0038, 0071, 0074, 0088−0090, 0128, 0170.

[37**]** Estação Ecológica de Boracéia, Salesópolis, SP, (-23.6333ºS, -45.8667ºW,850m), (*morph* = 54), (*mtDNA* = 6):

FMNH136932-136939, 145365, 145369–145372, 145381, 145382, MVZ182786–182791, 183054, 183064, 183065, 183067, MZUSP10034, 10035, 29274-29289, 6643, 9467, 9718–9726.

[40**]** Alto da Serra, Paranapiacaba, SP, (-23.7833ºS, -46.3167ºW, 800m), (*morph* = 5): BMNH5.5.2.2, 5.5.2.3, MZUSP1777, 1780, 2059.

[43**]** Bertioga, SP, (-23.8500ºS, -46.1500ºW, 8m), (*morph* = 1): MZUSP28401.

[44**]** São Miguel Arcanjo, Taquaral, SP, (-23.8833ºS, -47.9833ºW, 659m), (*morph* = 1): MZUSP3746.

[46**]** Fragmento Osasco, Tapiraí, SP, (-23.9078ºS, -47.4541ºW, 952m), (*morph* = 1): MZUSP (AB234).

[48**]** Morro da Mina, CBE, Ribeirão Grande, SP, (-24.0992ºS, -48.3653ºW, 900m), (*morph* = 51): FMNH143286, MVZ183045, 183047–183049, 183051–183053, MZUSP26878, 26893, 27249, 27320, 27325–27329, 27332, 27333, 27335–27342, 27344, 27345, 27348, 27350, 27353-27366, 27368, 27373–27376, 27384.

[48**]** Parque Estadual Fazenda Intervales (Carmo base), Capão Bonito, SP, (-24.0992ºS, -48.3653ºW, 700m), (*morph* = 4), (*mtDNA* = 5): MHNCI5137–5139, 5287.

[53**]** Castro, PR, (-24.7833ºS, -50.0000ºW,1000m), (*morph* = 1): MZUSP2501.

[54**]** Parque Estadual Pico Paraná, Campina Grande do Sul, PR, (-25.3056ºS, -49.0553ºW, 1600m), (*morph* = 12), (*mtDNA* = 11): MN78682–78684, 78686–78692, 78696, 78698.

[56**]** Taquari (Graciosa route) Quatro Barras, PR, (-25.3656ºS, -49.0769ºW, 936m), (*morph* = 13): MHNCI2211, 3121, 3053, 3059, 3060, 3065, 3072, 3080, 3093, 3058, 3064, 3095, 3100.

[57**]** Roça Nova (930-1150m), PR, (-25.3514ºS, -48.9039ºW, 950m), (*morph* = 17), (*mtDNA* = 5): FMNH18177, BMNH3.7.1.41–3.7.1.50, MN74094, 74092, 74076, 74068, 74086, 74089.

[58**]** Mananciais da Serra, Piraquara, PR, (-25.4333ºS, -49.0553ºW, 900m), (*morph* = 4), (*mtDNA* = 1): MHNCI3078, 3098, 3105, MN78455.

[60**]** Guaricana, São José dos Pinhais, PR, (-25.5347ºS, -49.2064ºW, 907m), (*morph* = 13): MHNCI1550, 1551, 1553, 1564, 1570, 1572, 1577, 1583, 1597, 1614, 1628, 1649, 1660.

[62**]** Caraguatay, Misiones province, Argentina, (-26.6167ºS, -54.7667ºW, 192m), (*morph* = 1): FMNH26818.

[63**]** Morro da Igreja, Urubici, SC, (-25.4417ºS, -49.0633ºW, 1700m), (*morph* = 2), (*mtDNA* = 2): MN78593, 78602.

[64**]** Parque Nacional Aparados da Serra, RS, (-28.015ºS, -49.5917ºW, 1000m), (*morph* = 4), (*mtDNA* = 3): MN78488, 78513, 78562, 78564.

[65**]** Parque Nacional Serra Geral, Cambará do Sul, RS, (-29.0736ºS, -49.9944ºW, 1021m), (*morph* = 2), (*mtDNA* = 1): MN78501, 78540.

[66**]** Taquara do Mundo Novo, Rio Grande do Sul state, (-29.6506ºS, -50.78056ºW, 57m), (*morph* = 4): BMNH84.2.8.37, 84.2.8.38, 86.9.16.3, 86.9.16.4.

Delomys sublineatus

[1**]** Conceição do Mato Dentro, km14 (Mata do Dr. Daniel), MG, (-19.0372ºS, -43.425ºW, 700m), (*morph* = 1): MN3653.

[2**]** Forest Reserve Nova Lombardia, ES, (-19.9356ºS, -40.6003ºW, 800m), (*morph* = 4): MN (M-228, M-257), MN69551, 69558.

[3**]** Santa Teresa (includes Caixa D'Água, Goipapoaçu), ES, (-19.9356ºS, -40.6003ºW, 800m), (*morph* = 14): MN (M116, M118, M85, M90, M97), MN5270, 5366. 69544–69549, 69561.

[4**]** Mata do Sossego, Simonésia, MG, (-20.1239ºS, -42.0014ºW, 591m), (*morph* = 1), (*mtDNA* = 1): UFES-CTA 975.

[5**]** Sitio Pedreiras, Pedra Azul, Domingos Martins, ES, (-20.405ºS, -41.0031ºW, 1000m), (*morph* = 1), (*mtDNA* = 1): MN78993.

[7**]** Parque Estadual Forno Grande, Castelo, ES, (-20.5222ºS, -41.1047ºW, 1000m), (*morph* = 7): MBML2530, 2621, 2624, 2681, MN32677, 32685, 32816.

[8**]** Castelinho, Cachoeiro do Itapemirim, ES, (-20.6000ºS, -41.2000ºW, 800m), (*morph* = 1): MN69553.

[9**]** Parque Estadual Serra do Brigadero (Fazenda Brigadeiro), MG, (-20.6068ºS, -42.4100ºW, 1200m), (*morph* = 3), (*mtDNA* = 2): MZUFV1615–1617.

[10**]** Parque Estadual Serra do Brigadeiro (Fazenda Neblina), MG, (-20.7159ºS, -42.4868ºW, 1300m), (*morph* = 10), (*mtDNA* = 5): MZUFV554, 623, 678, 1137–1140, 1205, 1236.

[11**]** Engenheiro Reeve, ES, (-20.7667ºS, -41.4667ºW, 100m), (*morph* = 1): BMNH3.9.4.58.

[12**]** 4km N Castelinho, Cachoeiro Itapemirim, ES, (-20.8489ºS, -41.1128ºW, 1000m), (*morph* = 1): MN69559.

[13**]** Parque Estadual do Desengano, Santa Maria Madalena, RJ, (-21.9553ºS, -42.0081ºW, 1750m), (*morph* = 1): MN28693.

[14**]** Sumidouro (Faz. São José da Serra, estrada Teresópolis-Friburgo RJ 30), RJ, (-22.0497ºS, -42.6747ºW, 1000m), (*morph* = 8): MN31361–31364, MVZ200407–200410.

[15**]** Nova Friburgo, RJ, (-22.2819ºS, -42.5311ºW, 846m), (*morph* = 3): MN44060, 44061, 70045.

[16**]** Serra de Macaé, RJ, (-22.31667ºS, -42.3333ºW, 823m), (*morph* = 2): MZUSP2790, 2791.

[22**]** Faz. Boa Fé and C. Guinle, Teresópolis, RJ, (-22.4122ºS, -42.9656ºW, 871m), (*morph* = 20): FMNH53873, MN6335, 6347, 6992–6996, 6998, 6999, 7006, 7054, 7056, 7058–7060, 7090, 7091, 7093, 7095.

[24**]** Teresópolis, RJ, (-22.4333ºS, -42.9833ºW, 952m), (*morph* = 4): FMNH26596–26598, 26872.

[26**]** Parque Nacional da Serra dos Órgãos (base), Teresópolis, RJ, (-22.4547ºS, -42.9972ºW, 1200m), (*morph* = 3), (*mtDNA* = 1): MN70007, 70022, 70017.

[32] Parque Nacional da Bocaina, São José do Barreiro, SP, (-22.7199ºS, -44.6150ºW, 1400m), (*morph* = 1), (*mtDNA* = 1): MN (HGB DB10).
[35] Serra da Cantareira, SP, (-23.4603ºS, -46.6303ºW, 779m), (*morph* = 1): MZUSP6370.
[36] Casa Grande, Biritiba Mirim, SP, (-23,5725ºS, -46,0386ºW, 850m), (*morph* = 7): MN32449, UFMG0099−0111, 0190, 0864, 0873.
[37] Estação Ecológica de Boracéia, Salesópolis, SP, (-23.6333ºS, -45.8667ºW, 935m), (*morph* = 7), (*mtDNA* = 4): FMNH136931, 141628, 141629, 145383, MVZ183075, 183076, MZUSP10214.
[38] Caucaia do Alto (Reserva Morro Grande), SP, (-23.6878ºS, -47.0217ºW, 900m), (*morph* = 18), (*mtDNA* = 10): FMNH143287, MN78638, 78644, 78652, 78657, 78660, 78664, 78665, 78668, 78671, 78674, 78676, 78681, MVZ182796, MZUSP9778, 9898, 9913, 21830.
[39] Paranapiacaba, SP, (-23.7781ºS, -46.3044ºW, 820m), (*morph* = 1): MZUSP9920.
[41] Serra de Paranapiacaba (Alto da Serra), SP, (-23.7833ºS, -46.3167ºW, 800m), (*morph* = 3): MZUSP1776, 1778, 9918.
[42] Fragmento Fuzuê, Piedade, SP, (-23.8442ºS, -47.4512ºW, 1000m), (*morph* = 1): MZUSP (AB259).
[45] Fragmento Bicudinho, Piedade, SP, (-23.8859ºS, -47.4837ºW, 925m), (*morph* = 1): MZUSP (AB281).
[47] Tapiraí, SP, (-23.9636ºS, -47.5072ºW, 875m), (*morph* = 1): MZUSP (LNT10).
[48] Parque Estadual Intervales, Capão Bonito, SP, (-24.0992ºS, -48.3653ºW, 700m), (*morph* = 19): MVZ183050, 183069, 183073, 183074, MZUSP27319, 27323, 27324, 27330, 27331, 27346, 27347, 27351, 27371, 27372, 27519, 29306−29309.
[49] Fazenda Sakamoto, Campinho, Capão Bonito, SP, (-24.1791ºS, -48.2387ºW, 932m), (*morph* = 2), (*mtDNA* = 2): MZUSP (AB109, 111).
[50] Vale do Ribeira, SP, (-24.6667ºS, -47.4000ºW, 100m), (*morph* = 1): MHNCI2626.
[51] Barra de Icapara, SP, (-24.6828ºS, -47.4667ºW, 10m), (*morph* = 2): MZUSP21837, 21838.
[52] Iguape, SP, (-24.7019ºS, -47.9167ºW, 3m), (*morph* = 3), (*mtDNA* = 2): MZUSP22801, 26777, 26802.
[59] Antonina, PR, (-25.4500ºS, -48.7167ºW, 120m), (*morph* = 1): MHNCI3090.
[61] Hansa, SC, (-26.4333ºS, -49.2333ºW,75m), (*morph* = 3): BMNH28.10.11.29−28.10.11.31.

TABLE A1. Cytochrome *b* haplotypes and specimens of *Delomys* and outgroup taxa used in phylogenetic analyses. Specimens marked with an asteristic were karyotyped.

Species	Haps	GenBank number	Base pairs	Specimens	Karyotype	Karyotype source
D. altimontanus	1	KF316968	1143	MN69592*, PH10088, PH10027	2n=82/FN=86	this study
	2	KF316970	1143	MN60573*	2n=82/FN=86	this study
	3	KF316971	1143	LG205	–	–
	4	KF316975	1143	MN60575*, MN69712*	2n=82/FN=86	this study
	5	KF316972	1143	MN60585*	2n=82/FN=86	this study
	6	KF316973	1143	LG106	–	–
	7	KF316967	1143	PH10756, PH10079, PH10024, PH10190	–	–
	8	KF316969	1143	SGM21	–	–
	9	KF316974	1143	MN60576*	2n=82/FN=86	this study
D. dorsalis	10	KF317001	801	MVZ183056, MVZ192894, MVZ182789	–	–
	11	KF317027	801	MN70028, MN70150	–	–
	12	KF316989	801	MN70029	–	–
	13	KF316990	801	MN44066 (SO16)	–	–
	14	KF316998	801	HGB-DB18	–	–
	15	KF316992	801	MN70127	–	–
	16	KF316993	801	MN70128	–	–
	17	KF316994	801	MN70152	–	–
	18	KF316999	801	EEB711	–	–
	19	KF317000	801	EEB712	–	–
	20	KF317002	801	MVZ183054	–	–
	21	KF317003	801	MVZ192895	–	–

.....continued on the next page

TABLE A1. (Continued)

Species	Haps	GenBank number	Base pairs	Specimens	Karyotype	Karyotype source
	22	KF316976	801	MN80378*, MN80393	2n=82/FN=80	this study
	23	KF317004	801	MVZ182787	–	–
	24	KF316977	801	MN80396	–	–
	25	KF317005	801	MVZ192890	–	–
	26	KF316978	801	MN80397	–	–
	27	KF316979	1143	MN80410	–	–
	28	KF316980	1143	MN80411	–	–
	29	KF316981	1143	MN80415	–	–
	30	KF317006	801	MVZ192891	–	–
	31	KF317029	1143	MN44059*, MN44062*, HGB64*, MN78915*	2n=82/FN=80	this study; Geise *et al.* 2004
	32	KF316982	801	LG133*	2n=82/FN=80	Geise et al 2004
	33	KF316983	1143	MN60580	–	–
	34	KF316984	1143	MN60572, MN60588	–	–
	35	KF317030	1143	MN60578*, MN78927*	2n=82/FN=80	this study
	36	KF316985	1143	MN60579	–	–
	37	KF316986	1143	MN60586	–	–
	38	KF316991	801	HGB-DB20*	2n=82/FN=80	Geise et al 2004
	39	KF316995	801	UFMG1868	–	–
	40	KF316996	801	UFMG1868	–	–
	41	KF316997	801	UFMG1874	–	–
	42	KF316987	1143	MN60577*	2n=82/FN=80	this study
	43	KF316988	1143	MN60582, MN60583	–	–
	44	KF317031	1143	MN78909*, MN60581*, UFMG1875	2n=82/FN=80	this study
D. dorsalis	45	KF317021	801	MN78455*	–	–
	46	KF317028	801	MN78682*,MN74094,MN78684*,MN78696*	2n=82/FN=80	this study
	47	KF317023	801	MN78501*	2n=82/FN=80	this study
	48	KF317024	801	MN78540*	2n=82/FN=80	this study
	49	KF317025	801	MN78564*	2n=82/FN=80	this study
	50	KF317022	801	MN78593*, MN78602*	2n=82/FN=80	this study
	51	KF317007	801	MVZ183046, MVZ192912, MVZ192913	–	–
	52	KF317008	801	MVZ192911, MVZ195989	–	–
	53	KF317017	801	MN74076	–	–
	54	KF317018	801	MN74068	–	–
	55	KF317019	801	MN74086	–	–
	56	KF317020	801	MN74089, MN74092	–	–
	57	KF317026	1143	MN78488*	2n=82/FN=80	this study
	58	KF317009	801	MN78683*	2n=82/FN=80	this study
	59	KF317010	801	MN78698*	2n=82/FN=80	this study

.....continued on the next page

TABLE A1. (Continued)

Species	Haps	GenBank number	Base pairs	Specimens	Karyotype	Karyotype source
	60	KF317011	801	MN78687*	2n=82/FN=80	this study
	61	KF317012	713	MN78688*	2n=82/FN=80	this study
	62	KF317014	662	MN78689*	2n=82/FN=80	this study
	63	KF317013	801	MN78690*	2n=82/FN=80	this study
	64	KF317015	801	MN78691*	2n=82/FN=80	this study
	65	KF317016	1143	MN78692*	2n=82/FN=80	this study
D. sublineatus	66	KF317050	1143	MN78644*,MN78652*,MN78669*, MN78670*, UFES-CTA975, MZUFV1138	2n=72/FN=90	this study
	67	KF317040	801	MN78638*	2n=72/FN=90	this study
	68	KF317052	801	MN78993, AB111	–	–
	69	KF317051	801	MN78657*, HGB10	2n=72/FN=90	this study
	70	KF317041	801	MN78664*	2n=72/FN=90	this study
	71	KF317042	801	MN78668*	2n=72/FN=90	this study
	72	KF317043	700	MN78671*	2n=72/FN=90	this study
	73	KF317039	801	MVZ183076, MVZ183075	–	–
	74	KF317034	801	MZUFV1139	–	–
	75	KF317053	801	MN70017, MVZ200403	–	–
	76	KF317035	1143	MZUFV1236*,MZUFV1250*,MZUFV1140*	2n=72/FN=90	this study
	77	KF317032	801	MZUFV1616*	2n=72/FN=90	Moreira *et al.* 2009
	78	KF317033	801	MZUFV1615*	2n=72/FN=90	Moreira *et al.* 2009
	79	KF317045	801	MVZ192857	–	–
	80	KF317036	801	MVZ192918, MZUSP29311	–	–
	81	KF317037	801	MVZ192919	–	–
	82	KF317038	801	MVZ192917, MZUSP29310	–	–
	83	KF317046	801	MVZ183074	–	–
	84	KF317047	801	MVZ183068	–	–
	85	KF317048	801	AB109	–	–
	86	KF317049	528	CIT278, CIT328	–	–
	87	KF317044	801	MVZ182796	–	–
S. xerampelinus		AF108706	1143	UMMZ3408	–	–
N. albigula		DQ179858	1143	NK17583	–	–
S. hispidus		AF108702	1143	BYU15259	–	–
P. xanthopygus		AY956739	1143	LCM 1737	–	–